PPAR Research

Biological Network Analysis of PPAR and Related Signaling Pathways 2021

Lead Guest Editor: Hongbao Cao
Guest Editors: Anastasia Nesterova and Sha Liu

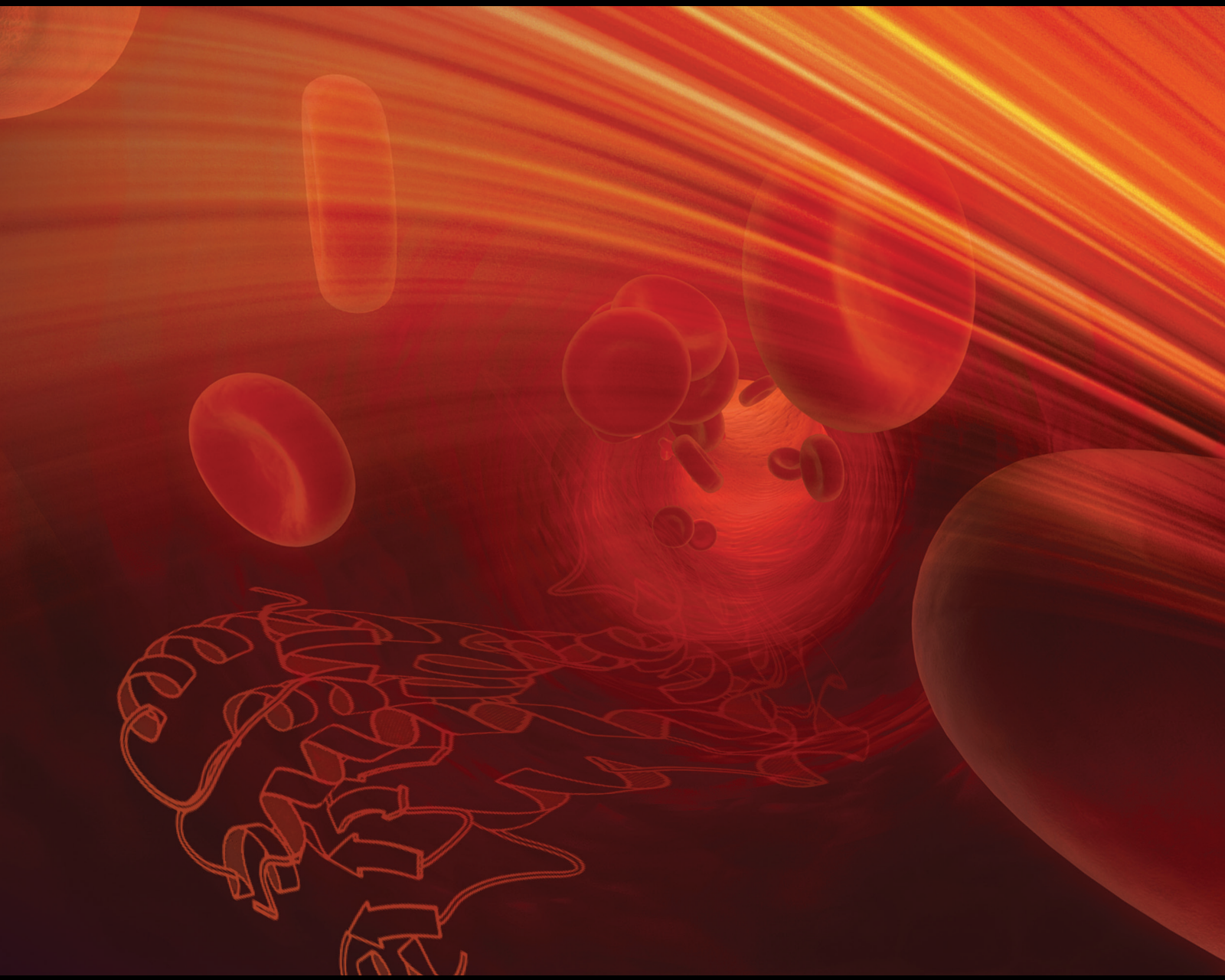

Biological Network Analysis of PPAR and Related Signaling Pathways 2021

PPAR Research

Biological Network Analysis of PPAR and Related Signaling Pathways 2021

Lead Guest Editor: Hongbao Cao
Guest Editors: Anastasia Nesterova and Sha Liu

Contents

Hindawi
PPAR Research
Volume 2022, Article ID 2054876, 7 pages
https://doi.org/10.1155/2022/2054876

Research Article

Explore the Role of the rs1801133-PPARG Pathway in the H-type Hypertension

Xiuwen Liang,[1] **Tingting He**,[2] **Lihong Gao**,[3] **Libo Wei**,[4] **Di Rong**,[5] **Yu Zhang**,[6] **and Yu Liu**[6]

[1]*Cardiology Department, Hulunbeir China Mongolia Hospital Affiliated to the Teaching Hospital of Inner Mongolia Medical University, No. 58 West Street, Hailar District, Hulunbuir, Inner Mongolia 021000, China*
[2]*Cardiology Department, Hulunbeir People's Hospital, No. 20, Shengli Street, Hailar District, Hulunbuir, Inner Mongolia 021008, China*
[3]*Neurology Department, Hulunbeir People's Hospital, No. 20, Shengli Street, Hailar District, Hulunbuir, Inner Mongolia 021008, China*
[4]*Cardiology Department, Inner Mongolia Medical University, No. 5 Xinhua Street, Huimin District, Hohhot, Inner Mongolia 010110, China*
[5]*Geriatric Department, Hulunbeir People's Hospital, No. 20, Shengli Street, Hailar District, Hulunbuir, Inner Mongolia 021008, China*
[6]*Cardiology Department, Inner Mongolia Minzu University, No. 536, West Huolinhe Street, Tongliao, Inner Mongolia 028000, China*

Correspondence should be addressed to Xiuwen Liang; 2019120254@stu.immu.edu.cn

Xiuwen Liang and Tingting He contributed equally to this work.

Received 11 January 2022; Revised 9 February 2022; Accepted 15 February 2022; Published 20 March 2022

Academic Editor: Hongbao Cao

Both rs1801133 mutation on Methylenetetrahydrofolate reductase (MTHFR) gene and transcription factor peroxisome proliferator-activated gamma (PPARG) have been associated with plasma homocysteine (Hcy) levels and hypertension. However, their role in H-type hypertension remains unclear. In this study, we first tested the association between rs1801133 genotypes and Hcy level in H-type hypertension using clinical profiles collected from 203 patients before and after the treatment using enalapril maleate and folic acid tablets (EMFAT). Then, we constructed a literature-based pathway analysis to explore the role of the rs1801133-PPARG signaling pathway in H-type hypertension and its treatment. Although presented similar blood pressure, the patients with TT genotype of rs1801133 were much younger (p value <0.05) and significantly higher in Hcy levels ($x^2 = 6.11$ and $p < 0.005$) than that in the CC and CT genotype groups. Pathway analysis showed that T-allele of rs1801133 could inhibit the expression of PPARG through the downregulation of folate levels and upregulation of Hcy levels, which increased the risk of hypertension and hyperhomocysteinemia. Treatment using EMFAT led to similarly decreased Hcy levels for all patients with different genotypes ($x^2 = 86.00$; $p < 0.36$), which may occur partially through the activation of PPARG. Moreover, even after treatment, the patients with TT genotype still presented significantly higher Hcy levels ($x^2 = 7.87$ and $p < 0.001$). Our results supported that rs1801133 mutation could play a role in H-type hypertension, which might be partially through the downregulation of PPARG. Moreover, PPARG might also be involved in treating H-type hypertension using EMFAT.

1. Introduction

H-type hypertension is essential hypertension accompanied by an elevated level of plasma homocysteine (Hcy) levels (≥10 μmol/L) [1]. Hcy levels typically are higher in men than in women and increase with age [2, 3]. Elevated levels of Hcy have been correlated with the occurrence of many disorders [4–6], including blood clotting and H-type hypertension [7, 8]. In China, the prevalence of hypertension is 29.6% [9], and about 75% of hypertensive patients present elevated homocysteine levels [10].

Hcy is a sulfur-containing amino acid derived from the metabolism of methionine and is metabolized by one of the two pathways: remethylation or transsulfuration. Methylenetetrahydrofolate reductase (MTHFR) is a key enzyme of homocysteine metabolism, providing a methyl group for Hcy remethylation into methionine and maintaining the normal levels of Hcy in the body [11]. Mutations of the MTHFR gene decrease MTHFR enzyme activity that prevents Hcy remethylation and increases Hcy levels in plasma [11, 12]. The MTHFR gene has at least two functional polymorphisms, 677T and 1298C. The MTHFR C677T (rs1801133) mutation is relatively common, which increases the risk of high Hcy levels [13].

Multiple studies have been conducted on the association between rs1801133 polymorphism and H-type hypertension. However, the results obtained remained controversial. For example, one recent clinical study involving 241 cases found a significant higher TT genotype prevalence in H-type hypertension patients (Hcy ≥ 15 μmol/L) than that in non-H-type hypertension patients (Hcy < 15 μmol/L), suggesting that TT variant of rs1801133 could be associated with H-type hypertension [11]. However, another recent study involving 185 patients found no association between the rs1801133 polymorphism and H-type hypertensive [8].

Peroxisome proliferator-activated receptor gamma (PPARG) is a type II nuclear receptor (protein regulating genes) encoded by the PPARG gene [14]. Many studies confirmed that PPARG plays a protective role in hypertension [15, 16]. Several studies also suggested that increased activity of PPARG could lower plasma Hcy [17], while hyperhomocysteinemia has been found to reduce the protein expression of PPARG [18, 19]. However, no study has reported a direct relationship between PPARG and H-type hypertension so far.

Here, we integrated clinical data analysis and large-scale literature-based pathway analysis to study the potential relation between PPARG and rs1801133 mutation and their potential role in the pathogenesis and treatment of H-type hypertension. Our results indicated that the rs1801133-PARG signaling pathway might be associated with H-type hypertension and play roles in its treatment using enalapril maleate and folic acid tablets (EMFAT).

2. Materials and Methods

The rest of this study was organized as follows. We first examined the relationship between different rs1801133 genotypes and plasma Hcy levels in H-type hypertension using clinical profiles collected from 203 patients. The treatment effect using EMFAT was also studied. Then, we conducted large-scale literature-based pathway analysis to construct signaling pathways and explore the relationship between rs1801133 mutation, PPARG, and H-type hypertension.

2.1. Clinical Data Collection. Clinical data were collected from newly diagnosed H-type hypertension patients diagnosed in Hulunbuir People's Hospital from October 2017 to October 2018. All patients met the standards of the China Guidelines for Prevention and Treatment of Hypertension (2010) with plasma Hcy ≥ 10 μmol/L. The inclusion criteria are as follows: the patients met the diagnostic criteria of type H hypertension. The Ethics Committee of HulunBuir Hospital approved the study, and all participants provided consent to participate after being informed of the study protocol. The exclusion criteria are as follows: all subjects with the following conditions were excluded, including secondary hypertension, malignant tumors, immune diseases, liver and kidney dysfunction (liver enzymes: 3 times higher than the normal range, blood creatinine > 256 μmol/L), and those who were taking the medications that may affect the levels of plasma Hcy within six months, such as folic acid, vitamins, methotrexate, and oral contraceptives.

In total, 203 patients passed the recruiting criteria and were included in this study. According to their MTHFR genotype, these 203 H-type hypertension patients were divided into three groups: CC (wild-type homozygous) group, CT (heterozygous) group, and TT (mutant allele homozygous) group. The basic demographic information of patients was recorded, including gender, age, and ethnicity. In addition, the clinical parameters were recorded and compared among groups, including Hcy, blood pressure (systolic blood pressure and diastolic blood pressure), blood lipids (including triglyceride TG and cholesterol TC), fasting blood glucose value, and carotid artery color Doppler ultrasound. All the patients were treated with oral EMFAT for three months, with the Hcy level measured before and after the treatment.

2.2. MTHFR Gene Determination. The polymerase chain amplification (PCR) and the MX3005p fluorescently labeled probes were used to detect the genotype of the 677C/T polymorphic sites of the MTHFR gene in clinical specimens. The whole gene DNA of the blood sample was extracted and detected by fluorescent PCR technology. The genotype of MTHFR in the sample was distinguished by the difference in fluorescence.

2.3. Determination of Plasma Hcy. The fasting venous blood was collected from patients. An enzymatic cycling assay for homocysteine was evaluated using a Roche Modular Analytics P800 automatic chemistry analyzer. Plasma Hcy was evaluated using a Roche Modular Analytics P800 chemistry analyzer. The kit was provided by Oursa Company.

2.4. Statistical Analysis. SPSS21.0 software was used for statistical analysis. The measurement data were described by the mean ± standard deviation ($\bar{x} \pm s$). A one-way ANOVA was used for comparison between groups that conformed

Table 1: Patient baseline characters.

Group	Number of cases (%)	Age	Gender		Ethnicity		
			F	M	Han	Mongolian	Others
CC	55 (27.09)	59.2 ± 13.5	26	29	43	9	3
CT	96 (47.29)	59.0 ± 14.0	62	34	73	17	6
TT	52 (25.62)	53.2 ± 12.6	26	26	45	5	2

Table 2: Comparison of measured indicators among the three groups.

	CC	CT	TT	χ^2	p
Blood glucose (mmol/L)	5.50 ± 0.44	6.11 ± 2.99	5.84 ± 1.14	0.61	0.873
CHOL (mmol/L)	4.87 ± 0.73	5.28 ± 1.00	5.49 ± 0.96	0.23	0.956
TG (mmol/L)	2.08 ± 1.42	1.47 ± 0.48	1.80 ± 0.59	1.28	0.298
SBP (mmHg)	150.59 ± 16.12	152.77 ± 15.41	151.60 ± 20.13	1.25	0.339
DBP (mmHg)	86.64 ± 16.84	82.00 ± 10.94	87.60 ± 9.63	1.37	0.279
Pre-Hcy (μmol/L)	14.26 ± 4.06	13.27 ± 2.98	25.00 ± 18.07	6.11	0.005
Post-Hcy (μmol/L)	11.52 ± 4.58	11.55 ± 2.40	18.22 ± 7.73	7.87	0.001
The changes of Hcy level	2.740 ± 2.40	1.71 ± 3.87	6.780 ± 14.20	86.00	0.360
The incidence rate of atherosclerotic changes in carotid color Doppler ultrasound (%)	27.3	54.5	30	2.994	0.224

to a normal distribution, the rank-sum test was used for comparison between groups that did not conform to a normal distribution, and X^2 test was used for count data. $p < 0.05$ was considered to be statistically significant.

2.5. rs1801133-PPARG Signaling Pathway for H-type Hypertension. Assisted by Elsevier Pathway Studio (version 12.4.0.3: database of functional relationships and pathways of mammalian proteins; Elsevier), an rs1801133-PPARG signaling pathway was constructed to explore the connection between rs1801133 mutation, PPARG, and their potential roles in the pathology and treatment of hypertension and hyperhomocysteinemia. The entities within the pathways include the two main components of enalapril maleate and folic acid tablets (folate and enalapril), C677T polymorphism (rs1801133) in the MTHFR gene, two diseases (hyperhomocysteinemia and hypertension), the protein PPARG, and the small molecule homocysteine. The relationship between the entities within the signaling pathway was supported by results published in previous studies, which covers the full PubMed abstracts and over 6.9M Elsevier and third-party full-text articles. The direction, polarity, and reliability of the relationships were manually checked as a quality control process. Following a similar approach, we also compiled the pathway to explore the influence of aging on H-type hypertension and its treatment.

3. Results

3.1. Patient Baseline Characteristics. The baseline characteristics of patients are presented in Table 1. A total of 203 patients diagnosed with H-type hypertension were included in this study, of which 114 were women and 89 were men. According to their MTHFR genotype, all the patients were divided into three groups, including 55 patients in the CC group, 96 in CT, and 52 in TT, respectively. CT type accounts for 47.29% of the total H hypertension patients, indicating that most patients have at least a partial mutation (p value < 0.05).

As shown in Table 1, the average ages of the CC, CT, and TT groups were 59.2 ± 13.5 years, 59.0 ± 14.0 years, and 53.2 ± 12.6 years, without significant differences among the three groups (p value > 0.05) as a whole. However, the average age of the CT group and CC group was significantly higher than that of the TT group (p value < 0.05), which indicated that the onset age of H-type hypertension patients might vary according to different rs1801133 phenotypes. For gender and ethnicity, no significant difference was found among the three groups (p value > 0.05). In addition, the blood pressure, blood lipids, blood glucose, and atherosclerotic changes were measured and compared among three genotype groups, with no significant difference detected (p value > 0.05; see Table 2). These findings suggested that ethnicity, gender, and the blood indicators (blood glucose, CHOL, and TG) of H-type hypertension patients may not associate with rs1801133 mutation.

3.2. The Relationship between the rs1801133 Polymorphism and Hcy Levels. The relationship between rs1801133 polymorphism and Hcy levels in the H-type hypertension patients was analyzed. The Hcy levels were measured for patients before and after treatment using EMFAT. As shown in Table 2, before treatment, the levels of Hcy in the CC group, CT group, and TT group were 14.26 ± 4.06, 13.27 ± 2.98, and 25.00 ± 18.07, respectively, showing significant association with rs1801133 polymorphism ($X^2 = 6.109$, $p =$

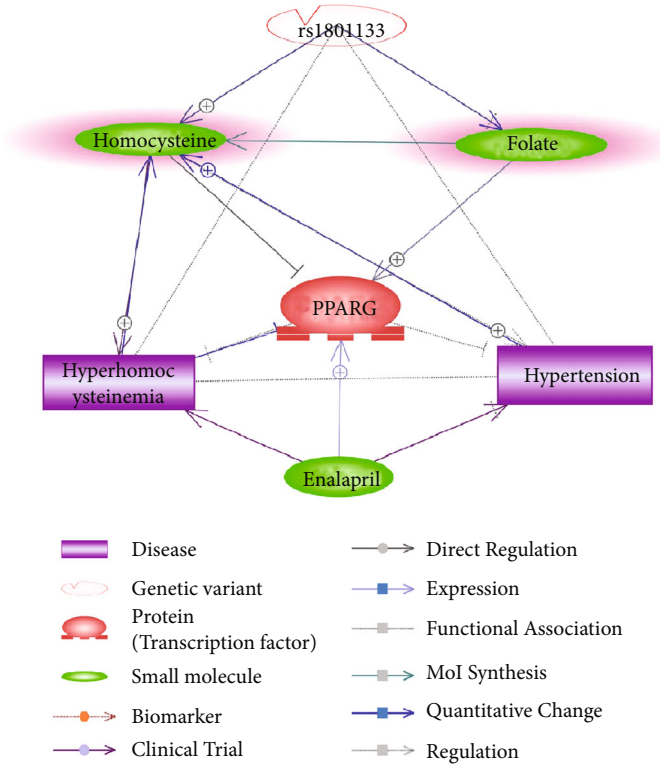

Figure 1: MTHFR-C677T-PPARG signaling pathway for H-type hypertension.

0.005). The level of Hcy in the TT group was significantly higher than that of the CC group and the CT group (p value < 0.05). These findings indicated that rs1801133 polymorphism was significantly related to the elevated Hcy levels in H-type hypertension patients.

All the patients in three different groups were treated with oral EMFAT (10 mg) once a day. After three-month treatment, the levels of Hcy in the CC group, CT group, and TT group were 11.52 ± 4.58, 11.55 ± 2.40, and 18.22 ± 7.73, which were significantly lower than those before treatment (p value < 0.05). To note, the treatment effect by using EMFAT was similar for all three groups in terms of decreasing the Hcy levels ($p = 0.36$). In addition, the between-group Hcy level differences remained high after the treatment ($p < 0.001$), which highlighted the impact of rs1801133 mutation on Hcy levels in H-type hypertension patients.

3.3. rs1801133-PPARG Signaling Pathway for H-type Hypertension. The signaling pathway constructed through literature data analysis is presented in Figure 1. The composed pathway demonstrated the possible linkage among rs1801133 mutation, PPARG, homocysteine, folate, enalapril, hyperhomocysteinemia, and hypertension. Specifically, it showed that rs1801133 mutation could promote plasma homocysteine and inhibit folate, which led to decreased PPARG expression and increased risk of hypertension and hyperhomocysteinemia. Meanwhile, treatment using folate and enalapril increased the mRNA level and expression of PPARG, which contributed to the decrease of plasma homocysteine levels and blood pressure. The pathway suggested that both rs1801133 mutation and PPARG could play a role in the pathological development of H-type hypertension. Moreover, it might add new insights into understanding the treatment effect of EMFAT on H-type hypertension.

3.4. Role of Aging in H-type Hypertension. As we noted that patients in the TT group were much younger than that in the CT and CC groups, we composed the pathway to explore the role of aging in the pathogenesis of H-type hypertension and its treatment. As shown in Figure 2, aging is a risk factor for increased homocysteine levels [20], decreased uric acid [21], and folate deficiency [22], which increases the risk of hypertension and hyperhomocysteinemia. The fact that younger patients in the TT group presented similar blood pressure as elder patients (TC and CC groups) might highlight the influence of higher Hcy levels on blood pressure.

Interestingly, Griffin et al.'s study using the rat model showed that enalapril not only prevented the increase in blood pressure but even abrogated the blood pressure increases with aging [23], which partially explains the treatment effect of H-type hypertension using EMFAT.

4. Discussion

MTHFR is the rate-limiting enzyme in the methyl cycle, which includes the conversion of homocysteine into methionine. The C677C to T mutation in the catalytic region of the MTHFR gene might induce valine to replace alanine, leading to the enzyme's thermolability and the inhibition of MTHFR activity, decreasing the transformation from 5,10-methyltetrahydrofolate to 5-methyltetrahydrofolate [24, 25]. As a result, the level of plasma Hcy increases and causes specific

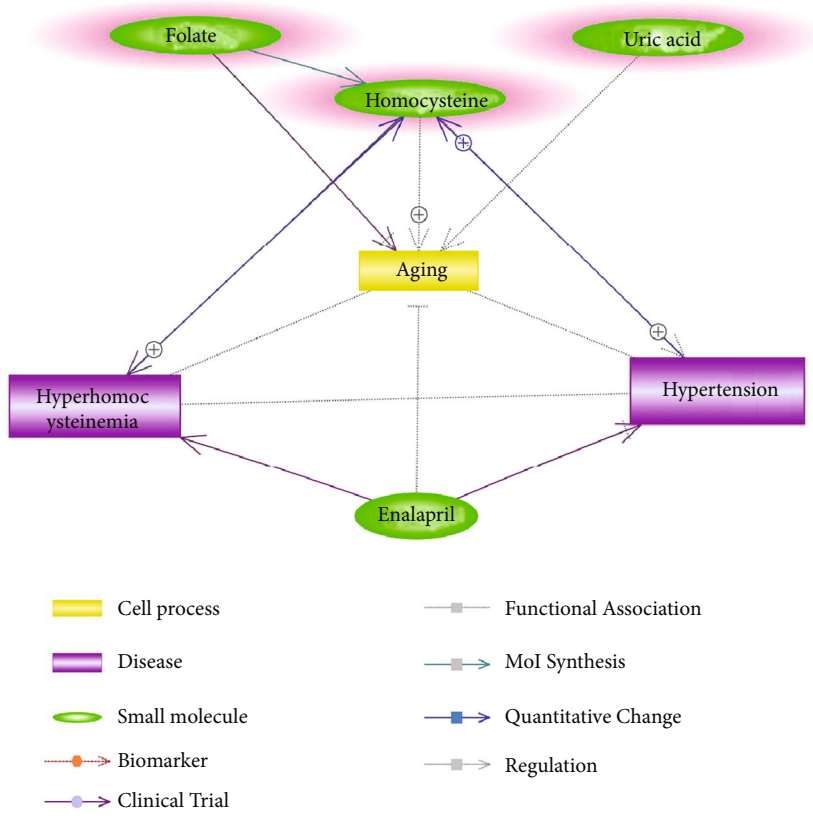

Figure 2: Pathway showing the role of aging in H-type hypertension and its treatment using enalapril maleate and folic acid tables.

pathological changes, including vascular endothelial damage, vascular smooth muscle proliferation, inhibition of nitric oxide production, and the development of hypertension [26–29].

In this study, the polymorphism of rs1801133 was analyzed in 203 H-type hypertension patients from the Hulunbuir region. The results indicated that 27.09% of patients were wild-type homozygous (CC), 47.29% were heterozygous (CT), and the remaining individuals (25.62%) were mutant allele homozygous (TT), indicating that most patients have heterozygous (CT) (p value < 0.05) (Table 1). To note, the distribution of CT genotype was similar to that in the previous study (49.95%) [30], which supported the validity of the clinical data employed in this study.

There was no difference in the distribution of rs1801133 genotypes based on sex and ethnicity (p value > 0.05), which was consistent with the report from the majority of previous studies [11]. However, we noted that patients in TT genotype were significantly younger than patients in CC or CT genotype group (p value < 0.05). Aging is the most common risk factor for the development of hypertension [31] and hyperhomocysteinemia [20], which was also implicated in the pathway presented in Figure 2. In other words, older rather than younger people are more susceptive to the risk of hypertension. Clinical data analysis showed that patients within TT genotype group presented significantly higher Hcy levels ($\chi^2 = 6.109$, $p < 0.005$ before treatment; $\chi^2 = 7.87$, $p < 0.001$ after treatment). Taken together, these results suggested that patients with TT genotype of rs1801133 were at a higher risk of developing hypertension at a younger age, which might be associated with the increased Hcy level. Our results suggested that the rs1801133 TT genotype was associated with H-type hypertension.

The literature-based pathway analysis (Figure 1) supported our clinical data analysis results that rs1801133 could lead to increased Hcy levels and decreased folic acid levels [30] and, therefore, could be a potential risk factor for H-type hypertension. Moreover, the influence of rs1801133 mutation on H-type hypertension may be partially through the inhibition of PPARG. On the one hand, homocysteine was an inhibitor of PPARG [19], which got promoted by rs1801133 TT mutation [30]. On the other hand, rs1801133 TT mutation decreases plasma folic acid [30], which was a promoter of PPARG [32]. Therefore, the mutation of rs1801133 could act as an inhibitor of PPARG. However, PPARG has been shown to play a protective role in hypertension [15] and has been demonstrated to lower plasma homocysteine [17]. In this sense, the downregulation of PPARG could partially explain the effect of rs1801133 mutation on the development of H-type hypertension.

Moreover, pathway analysis also showed that both major components of EMFAT, enalapril and folate, have been shown to unregulate PPARG [32, 33]. Therefore, as an inhibitor of hypertension and hyperhomocysteinemia, PPARG might also be involved in the treatment of H-type hypertension using EMFAT (Figure 1).

This study has several limitations that need future work. First, the clinical data were collected from the Hulunbuir

region with a limited sample size (203 patients), which may not represent H-type hypertension patients in general. Our results should be tested using more clinical data of larger size from different population regions. Second, the pathways built in this study were based on previous studies with different backgrounds. The pathways should be validated using data from the direct H-type hypertension study.

5. Conclusion

Our results support that rs1801133 mutation could play a role in the development of H-type hypertension, which may be partially through the downregulation of PPARG. Moreover, PPARG may also be involved in the treatment of H-type hypertension using EMFAT.

Data Availability

The data in our study are available from the corresponding author upon reasonable request.

Conflicts of Interest

The authors declare no conflict of interest.

Authors' Contributions

Xiuwen Liang and Tingting He contributed equally to this work.

Acknowledgments

This study was partially supported by the Hulunbuir City Science and Technology Bureau Scientific Research Program Project–Efficacy observation of enalapril maleate folic acid tablets on H-type hypertension patients with MTHFR gene polymorphism in the Hulunbuir area (Project No. 2018NS021).

References

[1] X. Qin and Y. Huo, "H-Type hypertension, stroke and diabetes in China: Opportunities for primary prevention," *Journal of Diabetes*, vol. 8, no. 1, pp. 38–40, 2016.

[2] O. Nygård, S. E. Vollset, H. Refsum et al., "Total plasma homocysteine and cardiovascular risk profile. The Hordaland Homocysteine Study," *JAMA*, vol. 274, no. 19, pp. 1526–1533, 1995.

[3] H. Refsum, E. Nurk, A. D. Smith et al., "The Hordaland Homocysteine Study: a community-based study of homocysteine, its determinants, and associations with disease," *The Journal of Nutrition*, vol. 136, no. 6, pp. 1731S–1740S, 2006.

[4] A. Verkleij-Hagoort, J. Bliek, F. Sayed-Tabatabaei, N. Ursem, E. Steegers, and R. Steegers-Theunissen, "Hyperhomocysteinemia and MTHFR polymorphisms in association with orofacial clefts and congenital heart defects: a meta-analysis," *American Journal of Medical Genetics. Part A*, vol. 143A, no. 9, pp. 952–960, 2007.

[5] M. Cattaneo, "Hyperhomocysteinemia, atherosclerosis and thrombosis," *Thrombosis and Haemostasis*, vol. 81, no. 2, pp. 165–176, 1999.

[6] I. M. Graham, L. E. Daly, H. M. Refsum et al., "Plasma homocysteine as a risk factor for vascular disease. The European Concerted Action Project," *JAMA*, vol. 277, no. 22, pp. 1775–1781, 1997.

[7] J. Zhang, Y. Liu, A. Wang et al., "Association between H-type hypertension and asymptomatic extracranial artery stenosis," *Scientific Reports*, vol. 8, no. 1, p. 1328, 2018.

[8] L. Q. Hong, C. X. Wu, H. Q. Wei, and G. Xu, "Clinical characteristics of H-type hypertension and its relationship with the MTHFR C677T polymorphism in a Zhuang population from Guangxi, China," *Journal of Clinical Laboratory Analysis*, vol. 34, no. 11, article e23499, 2020.

[9] J. Wang, L. Zhang, F. Wang, L. Liu, H. Wang, and the China National Survey of Chronic Kidney Disease Working Group, "Prevalence, awareness, treatment, and control of hypertension in China: results from a national survey," *American Journal of Hypertension*, vol. 27, no. 11, pp. 1355–1361, 2014.

[10] X. Qin, J. Li, Y. Cui et al., "Effect of folic acid intervention on the change of serum folate level in hypertensive Chinese adults: do methylenetetrahydrofolate reductase and methionine synthase gene polymorphisms affect therapeutic responses?," *Pharmacogenetics and Genomics*, vol. 22, no. 6, pp. 421–428, 2012.

[11] J. Song, J. Hou, Q. Zhao et al., "Polymorphism of MTHFR C677T gene and the associations with the severity of essential hypertension in Northern Chinese population," *International Journal of Hypertension*, vol. 2020, no. 6, Article ID 1878917, 2020.

[12] A. Zaghloul, C. Iorgoveanu, A. Desai, K. Balakumaran, and K. Chen, "Methylenetetrahydrofolate reductase polymorphism and premature coronary artery disease," *Cureus*, vol. 11, no. 6, article e5014, 2019.

[13] P. F. Jacques, A. G. Bostom, R. R. Williams et al., "Relation between folate status, a common mutation in methylenetetrahydrofolate reductase, and plasma homocysteine concentrations," *Circulation*, vol. 93, no. 1, pp. 7–9, 1996.

[14] M. E. Greene, B. Blumberg, O. W. McBride et al., "Isolation of the human peroxisome proliferator activated receptor gamma cDNA: expression in hematopoietic cells and chromosomal mapping," *Gene Expression*, vol. 4, no. 4-5, pp. 281–299, 1995.

[15] S. Fang and C. D. Sigmund, "PPARγ and RhoBTB1 in hypertension," *Current opinion in nephrology and hypertension*, vol. 29, no. 2, pp. 161–170, 2020.

[16] A. R. Nair, S. D. Silva Jr., L. N. Agbor et al., "Endothelial PPARγ (peroxisome proliferator-activated receptor-γ) protects from angiotensin II-induced endothelial dysfunction in adult offspring born from pregnancies complicated by hypertension," *Hypertension*, vol. 74, no. 1, pp. 173–183, 2019.

[17] J. Golledge and P. E. Norman, "Relationship between two sequence variations in the gene for peroxisome proliferator-activated receptor-gamma and plasma homocysteine concentration. Health in men study," *Human Genetics*, vol. 123, no. 1, pp. 35–40, 2008.

[18] S. Meng, S. Ciment, M. Jan et al., "Homocysteine induces inflammatory transcriptional signaling in monocytes," *Frontiers in bioscience*, vol. 18, no. 2, pp. 685–695, 2013.

[19] X. Pang, J. Si, S. Xu, Y. Li, and J. Liu, "Simvastatin inhibits homocysteine-induced CRP generation via interfering with the ROS-p38/ERK1/2 signal pathway in rat vascular smooth muscle cells," *Vascular Pharmacology*, vol. 88, pp. 42–47, 2017.

[20] C. Ma, Y. Zhao, and Z. Liu, "Vitamin D provides benefit based on the proinflammatory effects of homocysteine in elderly patients with type 2 diabetes mellitus," *Clinical Therapeutics*, vol. 42, no. 10, pp. 2010–2020.e1, 2020.

[21] H. R. Massie, M. E. Shumway, and S. J. Whitney, "Uric acid content of Drosophila decreases with aging," *Experimental Gerontology*, vol. 26, no. 6, pp. 609–614, 1991.

[22] S. J. James, S. Melnyk, M. Pogribna, I. P. Pogribny, and M. A. Caudill, "Elevation in S-adenosylhomocysteine and DNA hypomethylation: potential epigenetic mechanism for homocysteine-related pathology," *The Journal of Nutrition*, vol. 132, no. 8, pp. 2361S–2366S, 2002.

[23] K. A. Griffin, I. Abu-Amarah, M. Picken, and A. K. Bidani, "Renoprotection by ACE inhibition or aldosterone blockade is blood pressure-dependent," *Hypertension*, vol. 41, no. 2, pp. 201–206, 2003.

[24] B. Wei, Z. Xu, J. Ruan et al., "MTHFR 677C> T and 1298A> C polymorphisms and male infertility risk: a meta-analysis," *Molecular Biology Reports*, vol. 39, no. 2, pp. 1997–2002, 2012.

[25] P. Frosst, H. J. Blom, R. Milos et al., "A candidate genetic risk factor for vascular disease: a common mutation in methylene-tetrahydrofolate reductase," *Nature Genetics*, vol. 10, no. 1, pp. 111–113, 1995.

[26] A. Tawakol, T. Omland, M. Gerhard, J. T. Wu, and M. A. Creager, "Hyperhomocyst (e) inemia is associated with impaired endothelium-dependent vasodilation in humans," *Circulation*, vol. 95, no. 5, pp. 1119–1121, 1997.

[27] S. Heux, F. Morin, R. A. Lea, M. Ovcaric, L. Tajouri, and L. R. Griffiths, "The methylentetrahydrofolate reductase gene variant (C677T) as a risk factor for essential hypertension in Caucasians," *Hypertension Research*, vol. 27, no. 9, pp. 663–667, 2004.

[28] Y. Y. Li, "Methylenetetrahydrofolate reductase C677T gene polymorphism and coronary artery disease in a Chinese Han population:a meta-analysis," *Metabolism*, vol. 61, no. 6, pp. 846–852, 2012.

[29] M. A. Alam, S. A. Husain, R. Narang, S. S. Chauhan, M. Kabra, and S. Vasisht, "Association of polymorphism in the thermolabile 5, 10-methylene tetrahydrofolate reductase gene and hyperhomocysteinemia with coronary artery disease," *Molecular and Cellular Biochemistry*, vol. 310, no. 1-2, pp. 111–117, 2008.

[30] E. S. Brilakis, P. B. Berger, K. V. Ballman, and R. Rozen, "Methylenetetrahydrofolate reductase (MTHFR) 677C>T and methionine synthase reductase (MTRR) 66A>G polymorphisms: association with serum homocysteine and angiographic coronary artery disease in the era of flour products fortified with folic acid," *Atherosclerosis*, vol. 168, no. 2, pp. 315–322, 2003.

[31] G. L. Bakris, E. Ritz, and World Kidney Day Steering Committee, "The message for World Kidney Day 2009: hypertension and kidney disease: a marriage that should be prevented," *JASH*, vol. 3, no. 2, pp. 80–83, 2009.

[32] F. H. Lv, J. Z. Gao, Q. L. Teng, and J. Y. Zhang, "Effect of folic acid and vitamin B12 on the expression of PPARγ, caspase-3 and caspase-8 mRNA in the abdominal aortas of rats with hyperlipidemia," *Experimental and Therapeutic Medicine*, vol. 6, no. 1, pp. 184–188, 2013.

[33] E. M. de Cavanagh, F. Inserra, and L. Ferder, "Angiotensin II blockade: how its molecular targets may signal to mitochondria and slow aging. Coincidences with calorie restriction and mTOR inhibition," *American Journal of Physiology. Heart and Circulatory Physiology*, vol. 309, no. 1, pp. H15–H44, 2015.

Hindawi
PPAR Research
Volume 2022, Article ID 9414524, 9 pages
https://doi.org/10.1155/2022/9414524

Research Article

Increased PPARD Expression May Play a Protective Role in Human Lung Adenocarcinoma and Squamous Cell Carcinoma

Yong Zhu,[1] **Yedong Mi**,[2] **Zhonghua Qin**,[2] **Xuewei Jiang**,[2] **Yibo Shan**,[2] **Kamil Kural**,[3] **and Guiping Yu**[2]

[1]*Department of Thoracic Surgery, The 9th People's Hospital of Suzhou, Suzhou, Jiangsu Province 215200, China*
[2]*Department of Cardiothoracic Surgery, Jiangyin People's Hospital Affiliated to Nantong University, No. 163 Shoushan Rd, Jiangyin, Jiangsu Province 214400, China*
[3]*School of Systems Biology, George Mason University, Manassas, VA 20110, USA*

Correspondence should be addressed to Guiping Yu; xiaoyuer97103@163.com

Received 26 August 2021; Revised 2 January 2022; Accepted 3 February 2022; Published 15 March 2022

Academic Editor: Sha Liu

Peroxisome proliferator-activated receptor-δ, encoded by gene *PPARD*, is overexpressed in a majority of human lung cancer subtypes, but its role in the tumor progression remains poorly understood. We have analyzed the expression of *PPARD* in lung adenocarcinoma (LA) and squamous cell carcinoma (LSCC) datasets. The potential roles of *PPARD* in the pathological development of LA and LSCC were explored through literature-based pathway analysis and pathway enrichment analysis. In all LA datasets ($N = 11$) and in seven out of nine LSCC studies, the levels of *PPARD* were increased as compared to control tissues (log-fold changes were 0.37 ± 0.20 and 0.10 ± 0.37 for LA and LSCC, respectively). On average, the expression levels of *PPARD* in LA were higher than those in LSCC ($p = 0.036$). Pathway analysis showed that the overexpression of PPARD might play both positive and negative roles in the development of both LA and LSCC. Specifically, *PPARD* inhibits seven LSCC promoters and seven LA promoters and activates one LSCC inhibitor and another LA inhibitor. However, PPARD also activates six and one promoters of LA and LSCC, respectively, which would facilitate the development of LA/LSCC. Our results suggested a mixed role of PPARD in LA/LSCC, which may add new insights into the understanding of the PPARD-lung cancer relationship.

1. Introduction

Lung carcinoma (LC) is a leading cause of cancer death worldwide [1]. Annually, lung cancer kills nearly 1.8 million people, more than breast, prostate, pancreatic, and colorectal cancers combined [2]. Lung cancer has been divided into two main histological types, namely, small-cell lung carcinoma (SCLC) and non-small-cell lung carcinoma (NSCLC) [3]. The latter is further subdivided into lung adenocarcinoma (LA), which comprises around 40% of all LC [1], and lung squamous cell carcinoma (LSCC) that accounts for about 30% of all lung cancer [1, 4].

Several previous studies suggested a strong association between the expression levels of peroxisome proliferator-activated receptor ß/d- (PPARD-) encoding gene and human lung cancer [5–8]. A majority of the studies found that *PPARD* is overexpressed in lung cancer [5, 8, 9], with one recent study pointing at the association of high expression levels of this gene with a worse prognosis [10]. However, the role that PPARD plays in the pathophysiology of lung cancer is far from being clear. Even if some studies unequivocally point at PPARD as a lung cancer-promoting gene [8], others suggest that ligand-driven activation of PPARD may suppress the growth of lung cancer [6] by inhibiting inflammation [7].

To facilitate our understanding of the role of the PPARD-encoding gene in lung cancer, we explored its activity of PPARD in expression dataset profiling major subtypes

of lung cancer, namely, LA and LSCC, and an influence of the increase in *PPARD* expression on the pathophysiology of LA and LSCC. We confirmed that in most cases of LA and LSCC, the expression of PPARD is increased, while its function may either enhance or suppress the proliferation of lung cancer depending on tissue context.

2. Method

The workflow of this study contains two significant sections. First, we collected publicly available gene expression datasets to explore and compare the expression changes of PPARD in the case of LA or LSCC. Then, we conducted large-scale literature data mining to build pathways connecting PPARD to LA or LSCC, revealing the potential role of PPARD in the pathological development of LA and LSCC.

2.1. Collection of Twenty Expression Datasets. To explore the expression activity of PPARD expression in LA and LSCC, we collected all available expression datasets within the Gene Expression Omnibus (https://www.ncbi.nlm.nih.gov/geo/). Keywords "lung adenocarcinoma" and "lung squamous cell carcinoma" were used for the dataset search. The data selection criteria were as follows: (1) the organism is Homo sapiens; (2) the data type is RNA expression by array; (3) the study has case vs. healthy control comparison; (4) the dataset and its format files are publically available; and (5) the datasets and its corresponding format files are publicly available. From each dataset, expression data for the healthy controls and LA/LSCC patients were extracted and reanalyzed.

2.2. PPARD Expression Analysis. To explore the PPARD expression within each independent study, instead of estimating an averaged expression value from all studies, we calculated and compared the PPARD expression log-fold change (LFC) for each dataset in the case of LA/LSCC compared to healthy controls. Multiple linear regression analysis has been conducted to explore the influence of multiple potentially influential factors on PPARD in the case of LA/LSCC, including sample population region (country), sample size, and sample profile collection date. Additionally, ANOVA has been used to compare the difference in expression patterns of PPARD between LA and LSCC cases.

2.3. PPARD-Driven Pathways Regulating LA/LSCC. To explore the potential influence of PPARD on LA/LSCC and improve our understanding of the underlying mechanisms, we conducted a large-scale literature data mining, based on which we built molecular pathways connecting PPARD and LA/LSCC. Specifically, we composed the pathways driven by LA/LSCC influencing the expression and activity of PPARD and the pathways driven by PPARD influencing the pathological development of LA and LSCC. The literature data mining was performed within the Pathway Studio (http://www.pathwaystudio.com) environment, which houses over 24 million PubMed abstracts and over 3.5 million Elsevier and third-party full-text papers. We initially identified the genes and functional classes that are downstream targets of PPARD and upstream regulators of LA/LSCC, manually reviewing the references and related sentences for quality control of each relationship identified. Relationships with no polarity or indirectly related to the activity of PPARD or human LA/LSCC were removed. The remaining relationships were used to construct the network describing the possible molecular pathways driven by PPARD to influence the pathological development of LA/LSCC.

2.4. Pathway Enrichment Analysis for LA/LSCC Regulators Driven by PPARD. To explore the functional profile of the PPARD-driven LA/LSCC regulators, we conducted a pathway enrichment analysis (PEA) using Pathway Studio. The input was the regulatory genes of LA/LSCC driven by PPARD. The background pathway database was Pathway Studio and Gene Ontology (GO) terms. These pathways/GO terms satisfy the false detective ratio analysis ($q = 0.005$) and also demonstrate an overlap of no less than 5% criteria.

3. Results

3.1. Expression of PPARD in LA/LSCC Datasets. A total of 20 lung cancer datasets qualified the inclusion criteria (Table 1). As shown in Figure 1, our results confirm that *PPARD* expression is increased in lung cancer, as its elevated levels were detected in all 11 LA datasets and seven out of 9 LSCC cases with log-fold changes 0.37 ± 0.20 and 0.10 ± 0.37 for LA and LSCC, respectively. Our findings are consistent with those reported previously. For the detailed results of the *PPARD* expression analysis, please refer to Supplementary Data (Expression Analysis) (available here).

In LA samples, average levels of PPARD expression were higher than those observed in LA ($p < 0.036$), Figure 1(b). The significant outliers of the PPARD expression were from datasets GSE32036 and GSE6706 which were displaying an opposite trend, which was driven by multiple outliers.

Due to a lack of relevant clinical information, we cannot determine the specific reason for the downregulation of PPARD expressions in these two datasets. However, we noted that the sample sources of dataset GSE32036 were NSCLC/SCLC cell lines using either Illumina HumanWG-6 V3 or HumanHT-12 V4. In dataset GSE67061, the PPARD expression profile was compared between LSCC lung tissue and normal airway epithelium cells. In comparison, most of the other datasets were comparing expression profiles acquired from the same source (e.g., disease/normal lung/bronchus of human). Therefore, we doubt the sample source could be a possible reason impacting the expression of PPARD in LSCC that needs further study.

3.2. LA/LSCC-Driven Pathways Regulating PPARD. To better understand the influence of LA/LSCC on the expression of PPARD, we conducted another literature-based pathway analysis, as shown in Figure 2. These pathways showed that LSCC demonstrated an overwhelming promotion effect on the expression of PPARD through the regulation of 10 out of 11 PPARD upstream regulators (highlighted in red in Figure 2(b). In contrast, LA presented a more complex effect on PPARD. Specifically, LA could exert a positive influence

Table 1: Key descriptors of 20 LA/LSCC RNA expression datasets selected for this study.

GEO ID	Disease name	*N* controls	*N* cases	Sampled population (country)	Time factor	Sample source
GSE7670	LA	28	27	Taiwan	13	Adenocarcinoma/normal lung
GSE68465	LA	4	443	USA	5	Adenocarcinoma/normal lung
GSE67061	LSCC	8	69	China	3	LSCC/normal airway epithelium cells
GSE63459	LA	32	33	USA	5	Adenocarcinoma/normal lung
GSE6044	LSCC	5	14	Germany	13	LSCC/normal lung
GSE51852	LA	4	49	Japan	6	Adenocarcinoma/normal lung
GSE46539	LA	92	92	Taiwan	4	Adenocarcinoma/normal lung
GSE43458	LA	30	80	USA	7	Adenocarcinoma/normal lung
GSE40791	LA	90	94	USA	7	Adenocarcinoma/normal lung
GSE33479	LSCC	27	14	USA	5	LSCC/normal bronchus
GSE32867	LA	58	58	USA	8	Adenocarcinoma/normal lung
GSE32036	LSCC	59	12	USA	7	NSCLC/SCLC cell lines
GSE31547	LA	20	30	USA	9	Adenocarcinoma/normal lung
GSE30219	LSCC	14	61	France	5	LSCC/normal lung
GSE19188	LSCC	65	27	Netherlands	9	LSCC/normal lung
GSE12472	LSCC	28	35	Netherlands	10	COPD bronchus/LSCC lung
GSE12428	LSCC	28	34	Netherlands	11	Normal bronchial/LSCC lung
GSE11969	LSCC	5	35	Japan	10	Adenocarcinoma/normal lung
GSE118370	LA	6	6	China	1	Adenocarcinoma/normal lung
GSE10072	LA	49	58	USA	12	Adenocarcinoma/normal lung

Note: "time factor" refers to the age of the dataset, which is defined by the current year–the publication year of the dataset.

on PPARD through 38 out of 49 PPARD upstream regulators, while LA may also inhibit PPARD through the regulation of 11 molecules.

3.3. MLR Results. Figure 1 presents the expression of PPARD variables among different studies. MLR results showed that the population region (country) of the samples could be a significant influential factor. In contrast, the sample size or the date of the sample profile collection has no significant effect (Table 2).

3.4. PPARD-Driven Pathways Affecting LA/LSCC. As shown in Figure 3, PPARD modulates multiple regulators of LA and LSCC to exert influence on the etiology and development of LA and LSCC. Specifically, PPARD inhibits seven LSCC promoters (THBS1, NOS2, TNF, ANG, MAPK8, MAPK9, and TGFBR family) and seven LA promoters (MYC, IL1B, TNF, KDR, MMP9, MMP2, and CDK1). In addition, PPARD activates one LSCC inhibitor (YAP1) and one LA inhibitor (TP53). PPARD drove these molecules to inhibit the pathological development and progression of LA/LSCC. These entities are highlighted in green in Figure 3.

Several LA/LSCC promoters that could be activated by PPARD were identified, including SIRT1, SOD1, LPCAT1, TWIST1, TGFB1, and SOD2 for LA and BCL2L1 for LSCC. Activation of these promoters could cause adverse effects that PPARD could exert on LA/LSCC. These molecules are highlighted in red in Figure 3. As a side note, PPARD drove different groups of regulators to influence LA and LSCC, with only one joint promoter (TNF).

3.5. PEA Results for LA/LSCC Regulators Driven by PPARD. To explore the functional profile of the PPARD-driven molecules that influence LA/LSCC, we performed three PEAS and presented the results in Figure 4. Detailed information of all the PEA results is provided in Supplementary Data: PEA4LA_Good, PEA4LA_Bad, and PEA4LSCC_Good, respectively (available here).

In Figure 4(a), we presented the top pathways/GO terms enriched by the molecules driven by PPARD (Figure 3(a)) to inhibit LA. Interestingly, besides the glial cell proliferation pathway, we also identified multiple vitamin D biosynthetic processes and regulation of calcidiol 1-monooxygenase activity-related pathways. A previous study showed that glial cell proliferation could promote the tumor cell growth of LA [11]. Moreover, vitamin D supplementation has been suggested as an approach to prevent lung cancer progression [12]. Regulation of these pathways may be part of the mechanism that PPARD may help to inhibit the progress of LA. In Figure 4(b), we presented the top pathways/GO terms enriched by the molecules driven by PPARD (Figure 3(a)) that could promote LA. Interestingly, most of these GO terms were related to superoxide, which is associated with tumor progression and migration in AFG1-induced LA [13, 14]. In Figure 4(c), we presented the pathways/GO terms enriched by the PPARD-modulated molecules that inhibit LSCC. The top two PEA results were related to podosome assembly, which has been shown to decrease the invasion and migration capabilities of LA cells [15]. The next two top GO terms

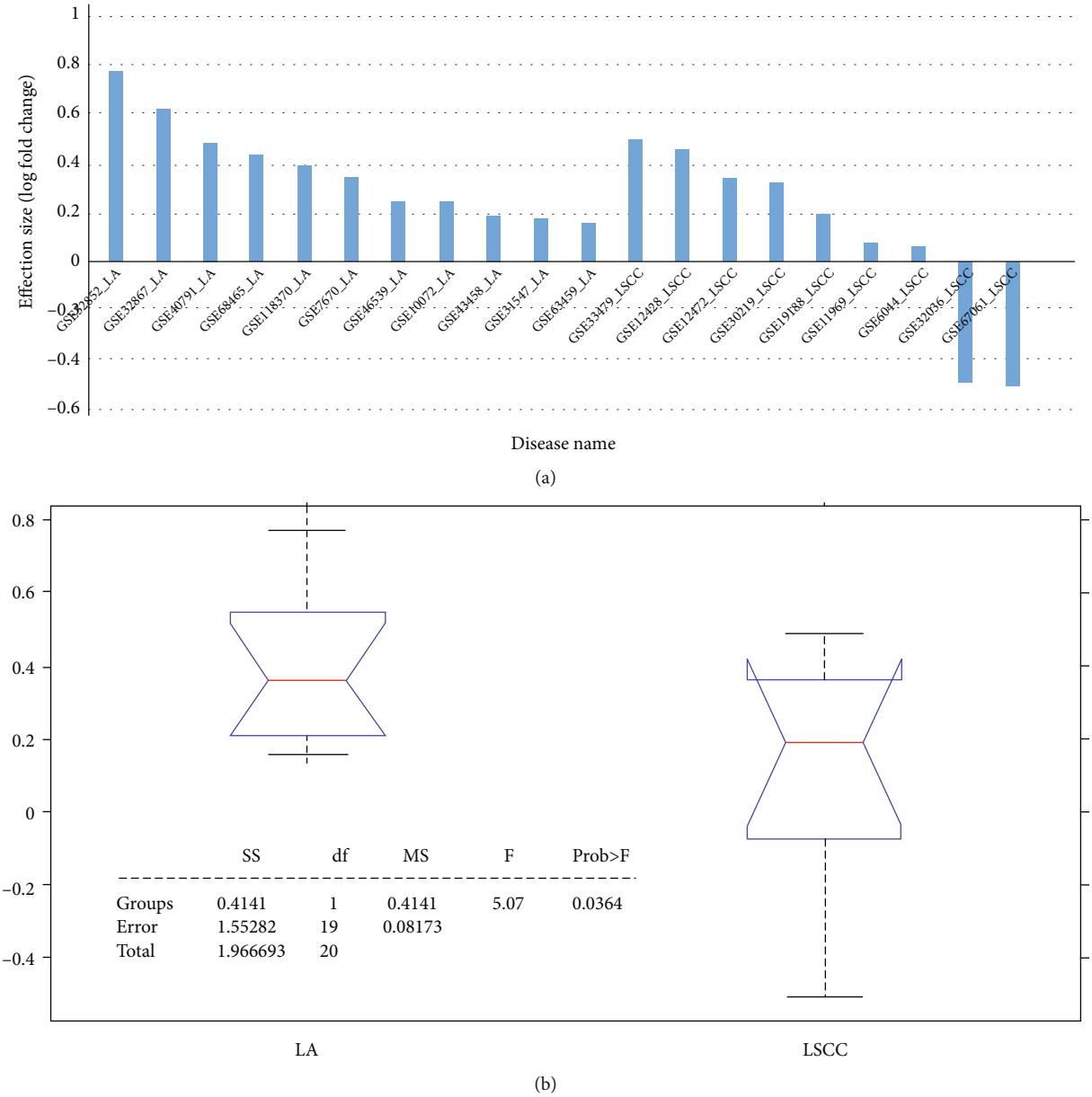

Figure 1: Expression of *PPARD* in 11 LA datasets and nine LSCC datasets: (a) bar plot of the expression log-fold change of PPARD; (b) boxplot of one-way ANOVA results.

were related to the transcription factor catabolic process, which has been shown to play vital roles in the development of human LA and LSCC [16, 17].

4. Discussion

Previous studies showed that gene PPARD demonstrated increased expression in patients with lung cancer [5, 8, 9]. However, there is a lack of discussion explaining PPARD overexpression in the etiology and development of lung cancer. In this study, we first explored the expression levels of PPARD in LA and LSCC, which account for about 70% of all lung cancer cases [1]; then, we employed a literature-based pathway analysis to explore the potential role of PPARD in LA/LSCC. Our results confirmed the overexpression of PPARD in most LA and LSCC cases. However, pathway analysis showed that the overexpression of PPARD might play a mixed role in the pathological development and progress of LA/LSCC.

Expression data analysis showed that PPARD demonstrated increased expression in 18 out of the 20 LA/LSCC independent datasets (Figure 1), which supported the previous finding that PPARD was overexpressed in the majority of lung cancers [5]. The two datasets, both were LSCC studies that presented decreased expression of PPARD, may be related to the specific drugs the patients were taking. Specifically, gene expression profiles in GSE32036 were collected from cell lines instead of patient tissues. For patients in GSE67061, the PPARD expression profile was compared between LSCC lung tissue and normal airway epithelium

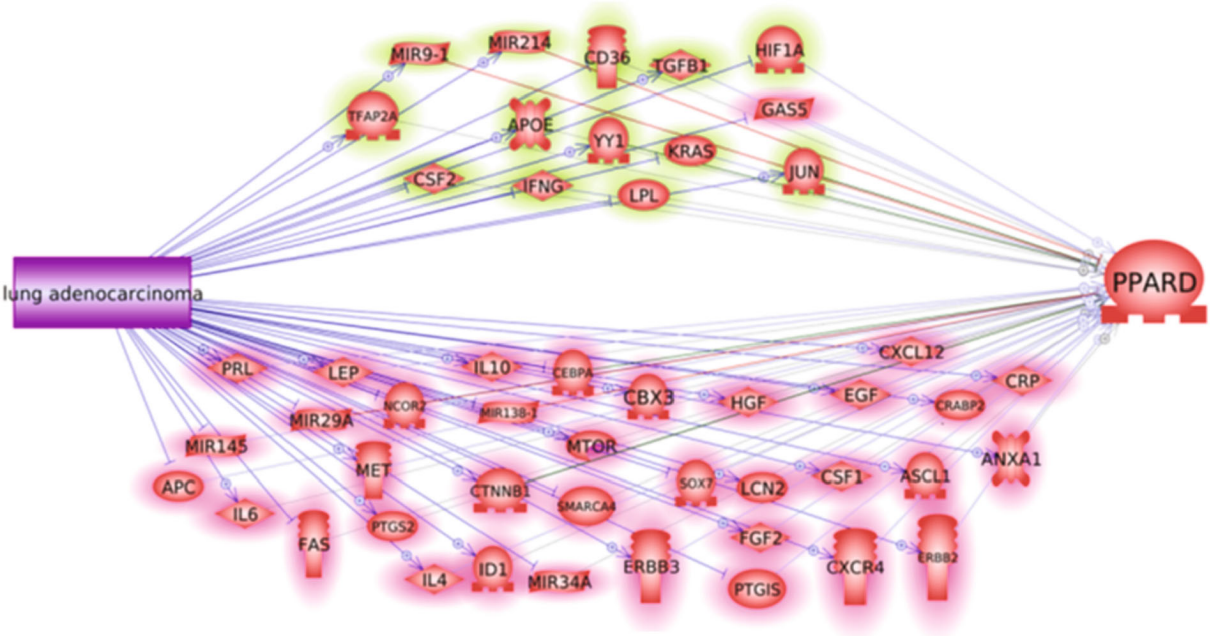

(a)

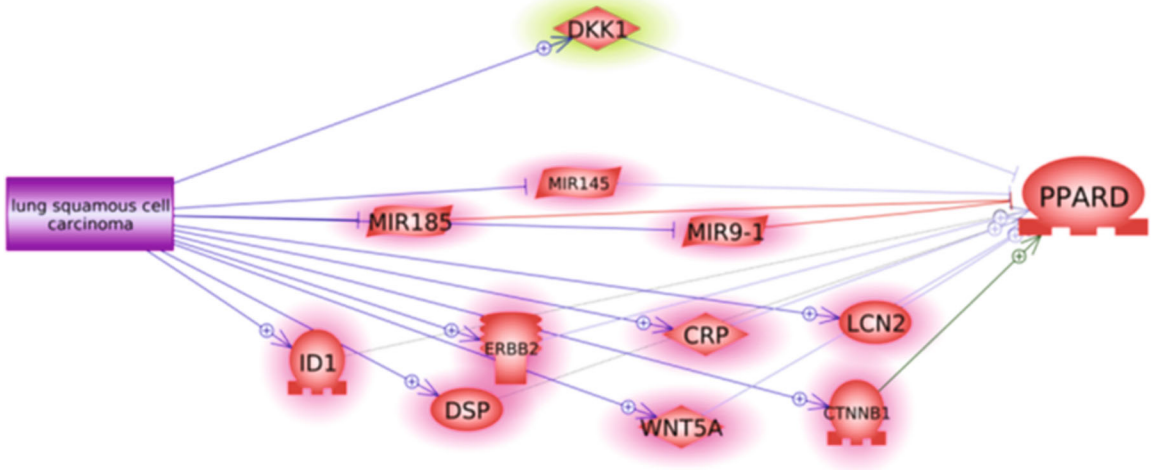

(b)

Figure 2: Pathways driven by LA/LSCC influencing the expression and activity of PPARD: (a) LA-driven pathway; (b) LSCC-driven pathway.

Table 2: Multiple linear regression analysis of three potential factors for PPARD expression in LA/LSCC.

	Sample #	Country	Study age
Beta	-1.97*E*-05	0.077	5.10*E*-4
Low limit	-1.63*E*-3	-0.01	-0.044
Up limit	1.59*E*-3	0.16	0.044
p value	0.51	0.015	0.49

cells [18]. However, due to a lack of relevant information, other factors that influence the expression of PPARD in the case of LA/LSCC should be studied. The complexity of the influence of LA and LSCC on PPARD was also demonstrated through the pathways in Figures 2(a) and 2(b), respectively. The upstream regulators of PPARD could be promoted or inhibited by LA and LSCC, through which both a negative and positive influence on the expression of PPARD could occur, which may partially explain the between-dataset expression variation of PPARD.

MLR results showed that the population region (country) of the samples could be a significant, influential factor (p value = 0.015; see Table 2). The sample size or the date of the sample profile collection did show a notable influence on the PPARD expression among the 20 LA/LSCC datasets. Moreover, ANOVA results showed that PPARD was more overexpressed in LA than in LSCC (Figure 1(b)). Even without the influence of two outliers (GSE32036 and GSE67061),

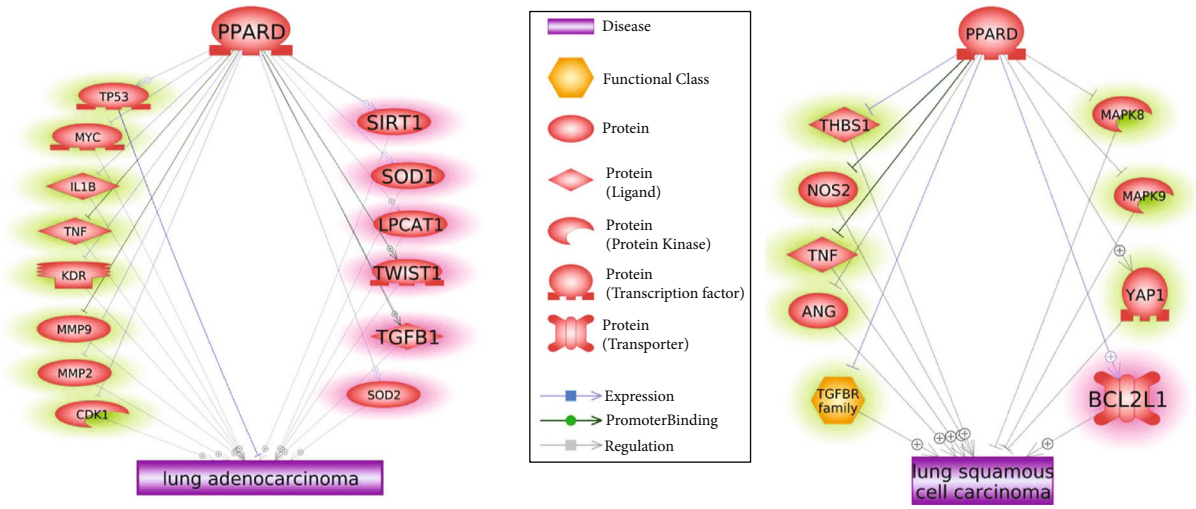

(a) (b)

Figure 3: Pathways driven by PPARD influencing the pathological development of LA and LSCC: (a) pathways connecting PPARD and LA; (b) pathways connecting PPARD and LSCC.

the overall PPARD expression in LSCC was still lower than that in LA (LFC = 0.270.17 and 0.370.20 for LSCC and LA, respectively). This may indicate a more prominent influence of PPARD on LA than on LSCC.

As shown in Figure 3, PPARD modulates multiple regulators of LA and LSCC to exert influence on the etiology and development of LA and LSCC. Specifically, PPARD inhibits seven LSCC promoters (THBS1, NOS2, TNF, ANG, MAPK8, MAPK9, and TGFBR family) and seven LA promoters (MYC, IL1B, TNF, KDR, MMP9, MMP2, and CDK1). For instance, THBS1 was found to promote tumorigenesis and invasion in LSCC [19], and macrophage inducible nitric oxide synthase (NOS2) promotes the initiation of LSCC [20]. Also, TNF has been shown to stimulate both LA and LSCC cells in mouse models [21]. We presented the detailed information of other LA/LSCC promoters in Supplementary Data: LSCC_PPARD Pathway and LA_PPARD Pathway (available here). By inhibiting these LA/LSCC promoters [22–24], the overexpression of PPARD could inhibit the initiation and progress of lung tumor cells.

In addition, PPARD activates one LSCC inhibitor (YAP1) and one LA inhibitor (TP53), which may be another mechanism of how PPARD could inhibit the pathological development of LA/LSCC. PPARD has also been shown to interact with YAP1 to promote gastric tumorigenesis [25], and YAP1 was suggested as a suppresser of LSCC through the reactivation of oxygen species accumulation [26]. Moreover, PPARD-induced P53 activation [27] has been shown to play a protective role in human LA [28, 29].

In addition, PPARD could also negatively influence the pathological development of LA/LSCC through the upregulation of the promoters of LA/LSCC. As shown in Figure 3(a), PPARD could activate six LA promoters and thereby facilitate the initiation and progression of LA. For example, PPARD agonist has been shown to increase SIRT1 protein levels [30], which is a tumor promoter in LA [31]. Activation of PPARD has also been associated with the increased expression of both SOD1 and SOD2 [32, 33], which are linked with tumor progression and migration in AFG1-induced LA [34]. Moreover, Weeden et al.'s study showed that it is necessary to inhibit both BCL2L1 and MCL1 [34] to induce tumor regression in LA sensitive to FGFR inhibition. However, PPARD has been shown to increase the expression of BCL2L1 [8], suggesting a PPARD-LSCC-promoting mechanism. For more of these vicious roles that PPARD could play in LA/LSCC, please see Supplementary Data: Ref4_LA_PPARD_Pathway and Ref4_LSCC_PPARD_Pathway (available here).

To note, PPARD drove different groups of regulators to influence LA and LSCC, with only one common promoter (TNF). This finding indicated that PPARD could exert influence on LA and LSCC through a different mechanism. PEA results showed that, on the one hand, LA might play a protective role against LA progression through the regulation of vitamin D biosynthetic process and glial cell proliferation [11, 12]. On the other hand, PPARD may modulate the response to oxygen radicals and superoxide to promote the development of LA [13, 14]. Moreover, PEA results also suggested that the mechanism that PPARD influences LSCC might be related to podosome assembly and the transcription factor catabolic process [15–17]. We provided the details of the pathways in Figure 4 and in Supplementary Data: PEA4LA_Good, PEA4LA_Bad, and PEA4LSCC_Good (available here).

Our study guaranteed several future works. First, in this study, we only used expression array data to study the expression of PPARD in LA/LSCC. Data of other modalities, including RNA sequencing data, should be used to validate this study's results. Second, besides sample population region, sample size, and sample profile collection date, more factors influencing the PPARD expression (e.g., age and gender) should be tested when data are available.

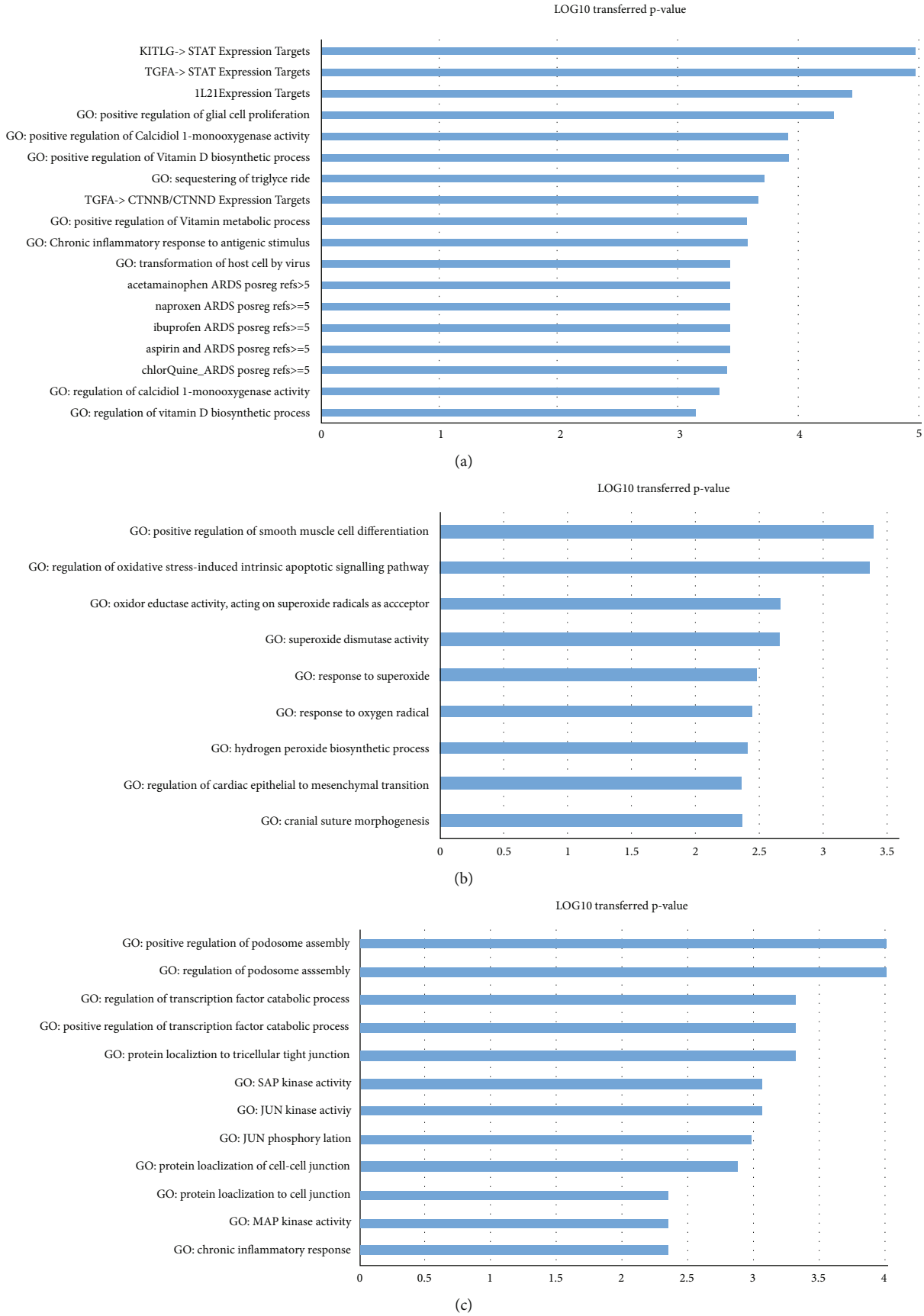

Figure 4: Pathway enriched analysis results: (a) the PEA results for eight PPARD-driven molecules to inhibit LA; (b) the PEA results for six PPARD-driven molecules to promote LA; (c) the PEA results for PPARD-driven LSCC regulators to inhibit LSCC.

5. Conclusion

Our results confirmed the increased gene expression of PPARD in the majority of cases of LA/LSCC. However, our pathway analysis indicated a mixed effect of the overexpression of PPARD on the pathological development and progression of LA and LSCC. The PPARD-driven pathways identified in our study may provide new insights into the understanding of the roles that PPARD plays in lung cancer.

Data Availability

The data in our study are available from the corresponding author upon reasonable request.

Conflicts of Interest

The authors declare no conflict of interest.

Authors' Contributions

Yong Zhu, Yedong Mi, and Zhonghua Qin contributed equally to this work.

Acknowledgments

This study was partially supported by the Wu Jieping Medical Foundation Special Fund for Clinical Research (Project ID: 320.6750.2020.10.45), the Open Project of Lung Cancer Sub-Bank of Jiangsu Major Disease Biological Resources Sample Bank (Project ID: SBK202004006); Project ID: P202102), the Scientific Research Project of Jiangsu Provincial Health Commission (Project ID: M2020076), the Wuxi "Double Hundred" Young and Middle-aged Medical and Health Top-notch Talents (Project ID: 147), and the Open Project of Jiangsu University Key Laboratory (Project ID: KY2019-037).

Supplementary Materials

The Supplementary Data is a multiworksheet Excel file that contains additional results described as follows: (1) Expression Analysis: the detailed results of the PPARD expression analysis in 11 LA datasets and 9 LSCC datasets that met the inclusion criteria; (2) Ref4_LSCC_PPARD Pathway: information regarding LSCC_PPARD Pathway was presented, including the type of the relationship, supporting references, and related sentences from the references where the relationship has been identified; (3) Ref4_LA_PPARD_Pathway: information regarding LA_PPARD Pathway was presented, including the type of the relationship, supporting references, and related sentences from the references where the relationship has been identified; (4) PEA4LA_Good: detailed information on all the PEA results that may inhibit the progress of LA; (5) PEA4LA_Bad: detailed information on all the PEA results that may promote the progress of LA; and (6) PEA4LSCC_Good: detailed information on all the PEA results that may inhibit the progress of LSCC. The excel file is online available at http://www.gousinfo.com/database/Data_Genetic/PPARD_Lung Cancer.xlsx. *(Supplementary Materials)*

References

[1] T. V. Denisenko, I. N. Budkevich, and B. Zhivotovsky, "Cell death-based treatment of lung adenocarcinoma," *Cell Death & Disease*, vol. 9, no. 2, p. 117, 2018.

[2] L. A. Torre, F. Bray, R. L. Siegel, J. Ferlay, J. Lortet-Tieulent, and A. Jemal, "Global cancer statistics, 2012," *CA: a Cancer Journal for Clinicians*, vol. 65, no. 2, pp. 87–108, 2015.

[3] F. Nasim, B. F. Sabath, and G. A. Eapen, "Lung cancer," *The Medical Clinics of North America*, vol. 103, no. 3, pp. 463–473, 2019.

[4] T. Sher, G. K. Dy, and A. A. Adjei, "Small cell lung cancer," *Mayo Clinic Proceedings*, vol. 83, no. 3, pp. 355–367, 2008.

[5] R. Müller, "PPARβ/δ in human cancer," *Biochimie*, vol. 136, pp. 90–99, 2017.

[6] P. He, M. G. Borland, B. Zhu et al., "Effect of ligand activation of peroxisome proliferator-activated receptor-β/δ (PPARβ/δ) in human lung cancer cell lines," *Toxicology*, vol. 254, no. 1-2, pp. 112–117, 2008.

[7] S. P. Lakshmi, A. T. Reddy, A. Banno, and R. C. Reddy, "PPAR agonists for the prevention and treatment of lung cancer," *PPAR Research*, vol. 2017, Article ID 8252796, 8 pages, 2017.

[8] T. V. Pedchenko, A. L. Gonzalez, D. Wang, R. N. DuBois, and P. P. Massion, "Peroxisome proliferator-activated receptor β/δ expression and activation in lung cancer," *American Journal of Respiratory Cell and Molecular Biology*, vol. 39, no. 6, pp. 689–696, 2008.

[9] Z. Yan, H. Zhang, C. Maher et al., "Prenatal polycyclic aromatic hydrocarbon, adiposity, peroxisome proliferator-activated receptor (PPAR) γ methylation in offspring, grand-offspring mice," *PLoS One*, vol. 9, no. 10, article e110706, 2014.

[10] X. Zuo, W. Xu, M. Xu et al., "Metastasis regulation by PPARD expression in cancer cells," *JCI Insight*, vol. 2, no. 1, article e91419, 2017.

[11] Y. W. Zang, X. D. Gu, J. B. Xiang, and Z. Y. Chen, "Brain metastases from colorectal cancer: microenvironment and molecular mechanisms," *International Journal of Molecular Sciences*, vol. 13, no. 12, pp. 15784–15800, 2012.

[12] T. Akiba, T. Morikawa, M. Odaka et al., "Vitamin D supplementation and survival of patients with non-small cell lung cancer: a randomized, double-blind, placebo-controlled trial," *Clinical Cancer Research*, vol. 24, no. 17, pp. 4089–4097, 2018.

[13] M. Romanowska, A. Maciag, A. L. Smith et al., "DNA damage, superoxide, and mutant K-ras in human lung adenocarcinoma cells," *Free Radical Biology & Medicine*, vol. 43, no. 8, pp. 1145–1155, 2007.

[14] T. C. Lo, F. M. Hsu, C. A. Chang, and J. C. Cheng, "Branched α-(1,4) glucans from Lentinula edodes (L10) in combination with radiation enhance cytotoxic effect on human lung adenocarcinoma through the Toll-like receptor 4 mediated induction of THP-1 differentiation/activation," *Journal of Agricultural and Food Chemistry*, vol. 59, no. 22, pp. 11997–12005, 2011.

[15] H. Zou, Q. Chen, A. Zhang et al., "MPC1 deficiency accelerates lung adenocarcinoma progression through the STAT3 pathway," *Cell Death & Disease*, vol. 10, no. 3, p. 148, 2019.

[16] T. Fukazawa, M. Guo, N. Ishida et al., "SOX2 suppresses _CDKN1A_ to sustain growth of lung squamous cell carcinoma," *Scientific Reports*, vol. 6, no. 1, p. 20113, 2016.

[17] T. Hussenet and S. du Manoir, "SOX2 in squamous cell carcinoma: amplifying a pleiotropic oncogene along carcinogenesis," *Cell Cycle*, vol. 9, no. 8, pp. 1480–1486, 2010.

[18] R. Tong, L. Feng, L. Zhang et al., "Decreased interferon alpha/beta signature associated with human lung tumorigenesis," *Journal of Interferon & Cytokine Research*, vol. 35, no. 12, pp. 963–968, 2015.

[19] P. V. Bommi, V. Chand, N. K. Mukhopadhyay, P. Raychaudhuri, and S. Bagchi, "NER-factor DDB2 regulates HIF1α and hypoxia-response genes in HNSCC," *Oncogene*, vol. 39, no. 8, pp. 1784–1796, 2020.

[20] Z. Gray, G. Shi, X. Wang, and Y. Hu, "Macrophage inducible nitric oxide synthase promotes the initiation of lung squamous cell carcinoma by maintaining circulated inflammation," *Cell Death & Disease*, vol. 9, no. 6, 2018.

[21] E. J. Ruiz, M. E. Diefenbacher, J. K. Nelson et al., "LUBAC determines chemotherapy resistance in squamous cell lung cancer," *The Journal of Experimental Medicine*, vol. 216, no. 2, pp. 450–465, 2019.

[22] M. Y. Ahn, S. A. Ham, T. Yoo et al., "Ligand-activated peroxisome proliferator-activated receptor δ attenuates vascular oxidative stress by inhibiting thrombospondin-1 expression," *Journal of Vascular Research*, vol. 55, no. 2, pp. 75–86, 2018.

[23] J. S. Welch, M. Ricote, T. E. Akiyama, F. J. Gonzalez, and C. K. Glass, "PPAR and PPAR negatively regulate specific subsets of lipopolysaccharide and IFN- target genes in macrophages," *Proceedings of the National Academy of Sciences of the United States of America*, vol. 100, no. 11, pp. 6712–6717, 2003.

[24] G. Ding, L. Cheng, Q. Qin, S. Frontin, and Q. Yang, "PPARδ modulates lipopolysaccharide-induced TNFα inflammation signaling in cultured cardiomyocytes," *Journal of Molecular and Cellular Cardiology*, vol. 40, no. 6, pp. 821–828, 2006.

[25] S. Song, Z. Wang, Y. Li et al., "PPARδ interacts with the Hippo coactivator YAP1 to promote SOX9 expression and gastric cancer progression," *Molecular Cancer Research*, vol. 18, no. 3, pp. 390–402, 2020.

[26] W. W. Pan, T. Moroishi, J. H. Koo, and K. L. Guan, "Cell type-dependent function of LATS1/2 in cancer cell growth," *Oncogene*, vol. 38, no. 14, pp. 2595–2610, 2019.

[27] K. J. Kim, J. H. Yun, J. I. Heo et al., "Role of pigment epithelium-derived factor in the involution of hemangioma: autocrine growth inhibition of hemangioma-derived endothelial cells," *Biochemical and Biophysical Research Communications*, vol. 454, no. 2, pp. 282–288, 2014.

[28] T. Koga, S. Hashimoto, K. Sugio et al., "Heterogeneous distribution of P53 immunoreactivity in human lung adenocarcinoma correlates with MDM2 protein expression, rather than withP53 gene mutation," *International Journal of Cancer*, vol. 95, no. 4, pp. 232–239, 2001.

[29] E. Barroso, E. Eyre, X. Palomer, and M. Vázquez-Carrera, "The peroxisome proliferator-activated receptor β/δ (PPARβ/δ) agonist GW501516 prevents TNF-α-induced NF-κB activation in human HaCaT cells by reducing p65 acetylation through AMPK and SIRT1," *Biochemical Pharmacology*, vol. 81, no. 4, pp. 534–543, 2011.

[30] X. Chen, D. Hokka, Y. Maniwa, C. Ohbayashi, T. Itoh, and Y. Hayashi, "Sirt1 is a tumor promoter in lung adenocarcinoma," *Oncology Letters*, vol. 8, no. 1, pp. 387–393, 2014.

[31] E. Ehrenborg and J. Skogsberg, "Peroxisome proliferator-activated receptor delta and cardiovascular disease," *Atherosclerosis*, vol. 231, no. 1, pp. 95–106, 2013.

[32] Y. C. Tseng, R. D. Chen, M. Lucassen et al., "Exploring uncoupling proteins and antioxidant mechanisms under acute cold exposure in brains of fish," *PLoS One*, vol. 6, no. 3, article e18180, 2011.

[33] L. Yi, H. Shen, M. Zhao et al., "Inflammation-mediated SOD-2 upregulation contributes to epithelial- mesenchymal transition and migration of tumor cells in aflatoxin G_1-induced lung adenocarcinoma," *Scientific Reports*, vol. 7, no. 1, p. 7953, 2017.

[34] C. E. Weeden, C. Ah-Cann, A. Z. Holik et al., "Dual inhibition of BCL-XL and MCL-1 is required to induce tumour regression in lung squamous cell carcinomas sensitive to FGFR inhibition," *Oncogene*, vol. 37, no. 32, pp. 4475–4488, 2018.

Hindawi
PPAR Research
Volume 2022, Article ID 4709300, 7 pages
https://doi.org/10.1155/2022/4709300

Research Article

Role of Apolipoprotein A1 in PPAR Signaling Pathway for Nonalcoholic Fatty Liver Disease

Changxi Chen,[1] **Hongliang Li**,[1] **Jian Song**,[1] **Cheng Zhang**,[1] **Mengting Li**,[1] **Yushan Mao**,[2] **Aiming Liu**,[3] **and Juan Du**[4]

[1]*Department of Gastroenterology, Affiliated People's Hospital of Ningbo University, Ningbo, Zhejiang Province 315040, China*
[2]*Department of Endocrinology, Affiliated Hospital of Medical College of Ningbo University, Ningbo, Zhejiang Province 315020, China*
[3]*School of Medicine, Ningbo University, Ningbo 315211, China*
[4]*Department of Gastroenterology, Refine-Chemical Hospital of Zhenhai District, Ningbo, Zhejiang Province 315207, China*

Correspondence should be addressed to Hongliang Li; lhlliang@sohu.com and Juan Du; juandu0132@163.com

Received 29 October 2021; Revised 27 November 2021; Accepted 14 December 2021; Published 18 February 2022

Academic Editor: Paul D. Drew

Peroxisome proliferator-activated receptors (PPARs) have been suggested to play crucial roles in the pathology of NAFLD with a vague understanding of the underlying mechanism. Here, we integrated large-scale literature data and clinical data to explore the potential role of the PPAR-APOA1 signaling pathway in the pathology of NAFLD. First, the signaling pathway connecting PPARs, APOA1, and NAFLD was constructed. Then, we employed clinical data to explore the association between APOA1 levels and NAFLD. In addition, we built the APOA1-driven pathway analysis to explore the potential mechanism of the APOA1-NAFLD association. Pathway analysis showed that APOA1 serves as a hubprotein connecting PPARs and NAFLD through a beneficial modulation of 16 out of 21 NAFLD upstream regulators. Each relationship within the composed pathway was supported by results from multiple previous studies. Clinical data analysis showed that an increase of APOA1 level was associated with a significantly decreased NAFLD prevalence ($\chi^2 = 292.109$; $P < 0.001$). When other confounding factors were adjusted, serum APOA1 level was shown as an independent risk factor for the prevalence of NAFLD (P value<.0001; OR = 0.562). Our results suggested that the three PPARs (PPARA, PPARD, and PPARG) might promote the expression and molecular transportation of APOA1 to form a PPAR-APOA1 signaling pathway that demonstrated a beneficial role in the pathogenesis of NAFLD.

1. Introduction

Nonalcoholic fatty liver disease (NAFLD) is characterized by an excessive fat build-up in the liver without a clear cause, such as alcohol use [1, 2]. NAFLD is also known as a metabolic dysfunction-associated fatty liver disease that has two subtypes, nonalcoholic fatty liver (NAFL) and nonalcoholic steatohepatitis (NASH). Compared with NAFL, NASH is more dangerous with liver inflammation [3]. NAFLD, especially when it progresses to NASH, may eventually lead to complications such as liver failure, liver cancer, cirrhosis, or cardiovascular disease [4].

Peroxisome proliferator-activated receptors have been suggested to play crucial roles in the pathology of NAFLD [5, 6]. Specifically, peroxisome proliferator-activated receptor δ (PPARD) and peroxisome proliferator-activated receptor α (PPARA) have been suggested as therapeutic targets to alleviate NAFLD [5, 7]. Peroxisome proliferator-activated receptor γ (PPARG) has also been shown essential to protect against nonalcoholic steatohepatitis [6]. However, the underlying mechanism regarding the roles of PPARs in NAFLD remains vague and controversial [8, 9].

As the major component of high-density lipoprotein (HDL) particles, apolipoprotein A1 (APOA1) is a protein encoded by the APOA1 gene to have a specific role in lipid metabolism [10, 11]. The APOA1 gene is located on the 11th chromosome, with its specific location being 11q23-q24. APOA1 is the major protein component of HDL

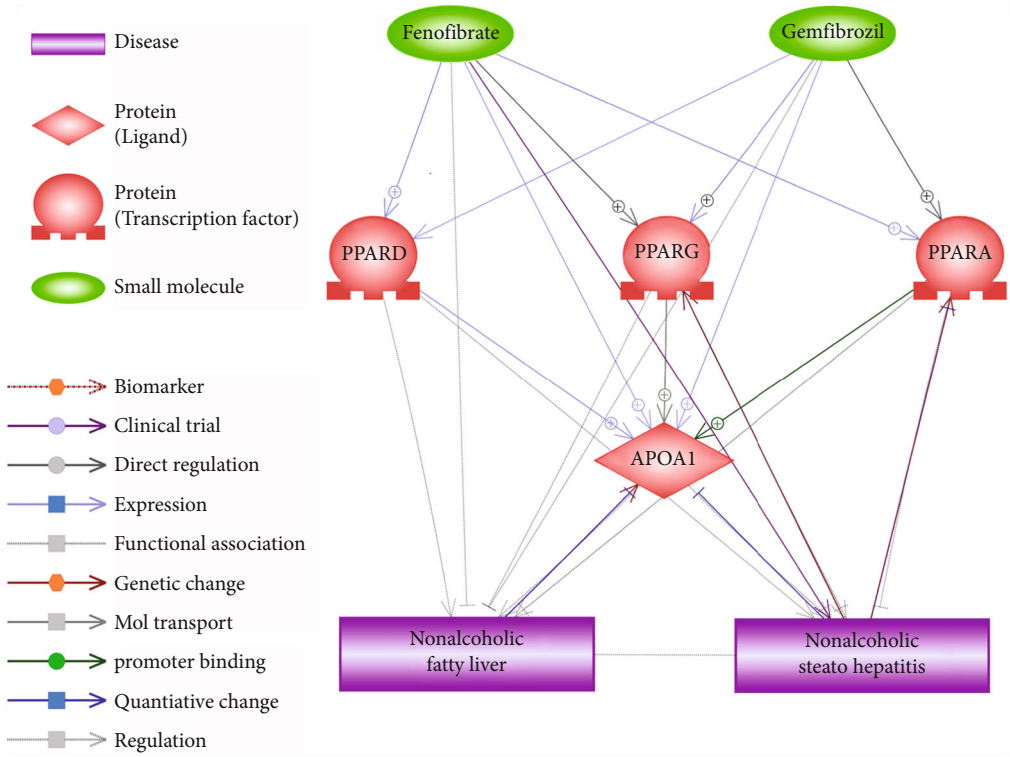

Figure 1: PPAR-APOA1 signaling pathway regulating nonalcoholic fatty liver disease.

particles in plasma; it enables efflux of fat molecules by accepting fats from within cells and transport elsewhere, including back to LDL particles or the liver for excretion. APOA1 helps clear fats from white blood cells within artery walls to keep from becoming fat overloaded, transforming into foam cells that contribute to progressive atheroma. It has been shown that APOA1 levels were significantly decreased in NAFLD patients [12], which increase the risk of NAFLD developing [13]. Ren et al.'s study found that both APOA1 and APOB and TC/HDL-C had the predictive value of NAFLD [14]. On the other hand, modulation of APOA1 activity leads to a beneficial effect on NASH [15].

All three PPARs (PPARA, PPARD, and PPARG) were implicated as promoters to increase APOA1 secretion and expression from the liver [16–18], which may partially decode the role of PPARs in NAFLD. Here, we employed large-scale literature-based pathway analysis and clinical data analysis to explore the role of the PPAR-APOA1 signaling pathway in NAFLD, which may add new insights into the understanding of the NAFLD treatment.

2. Materials and Methods

The rest of this study was organized as follows. First, we conducted a literature-based pathway analysis to study the PPAR-APOA1 signaling pathway and its role in the pathology of NAFLD. Second, we used large-scale clinical data to study the association between APOA1 levels and NAFLD. In addition, we constructed the genetic and small molecule pathways to explore the potential mechanism of APOA1-NAFLD association.

2.1. PPAR-APOA1 Signaling Pathway for NAFLD. Assisted by Elsevier Pathway Studio (http://www.pathwaystudio.com) knowledge database, we constructed the PPAR-APOA1 signaling pathway to explore the connection between PPARs, APOA1, and NAFLD. The entities within the network included the three PPARs (PPARA, PPARD, and PPARG), the protein APOA1, the diseases (nonalcoholic fatty liver and nonalcoholic steatohepatitis), and the two potential drugs for the treatment of NAFLD (fenofibrate and gemfibrozil). The relationships between the entities were identified by using the network building module (https://supportcontent.elsevier.com/Support%20Hub/Pathway%20Studio/Guide%20to%20Building%20Pathways%20in%20ChemEffect%20and%20DiseaseFX%20with%20Pathway%20Studio%20Web.pdf). The relationship between the entities within the signaling pathway was supported by at least three references. Then, a manual quality control process was conducted to ensure the reliability of the relationships. A reference list was provided in Supplementary Material 1, which is a two-worksheet excel file described as follows. The worksheet "Ref for PPARs-APOA1 pathway" contains reference information supporting the PPAR-APOA1 pathway (Figure 1), including the type of the relationship, supporting references, and related sentences from the references where the relationship has been identified. The worksheet "Ref for APOA1 Molecule pathway" contains reference information supporting the genetic and molecule pathways (Figure 2), including the type of the relationship, supporting

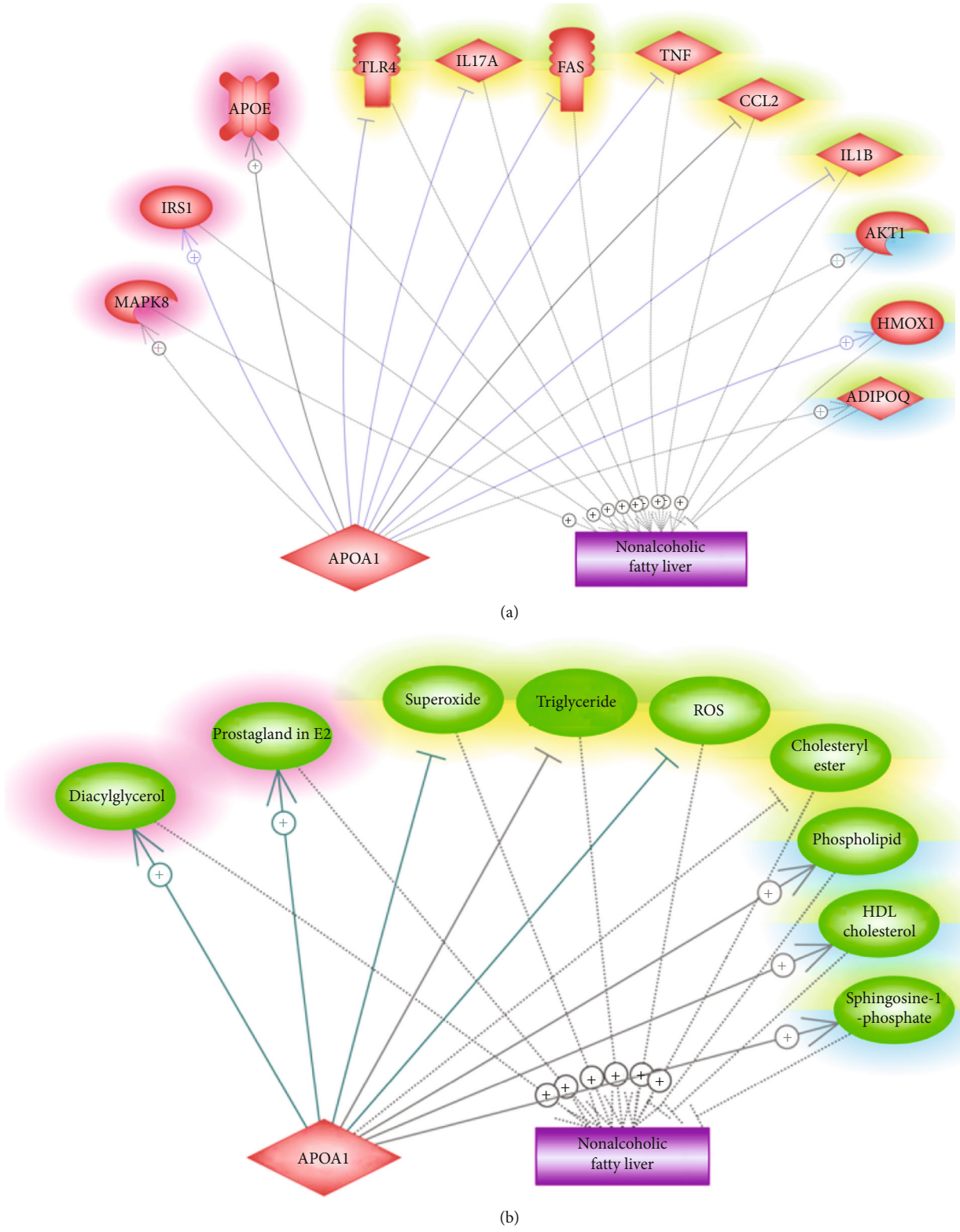

Figure 2: Molecule pathways that decode the APOA1-NAFLD relationship. (a) The APOA1-driven genetic pathway. (b) The APOA1-driven small molecular pathway.

references, and related sentences from the references where the relationship has been identified.

2.2. APOA1 Levels in NAFLD Clinical Data

2.2.1. Subjects in the Clinical Data. Clinical data were collected from inservice and retired employees who underwent physical examinations in the health examination center of Zhenhai Lianhua Hospital from March to November 2013.

Table 1: The prevalence of NAFLD decreased with the increase of APOA1 level.

APOA1 levels	Total patients	Patients with NAFLD	Prevalence rate	$\chi 2$ value	P value
Q1	3300	1075	32.58%	292.109	<0.001
Q2	3165	893	28.21%		
Q3	3156	680	21.55%		
Q4	3202	499	15.58%		

There were 14,320 questionnaires and physical examination forms with 257 undetected patients excluded, resulting in a total of 14,063 cases for physical examination; out of these 14,063 subjects, 1,240 subjects that met the exclusion criteria were removed from the data collection. Finally, a total of 12,823 subjects were included (8,479 males and 4,344 females). The average age was (47.2 ± 15.1) years. Of these 12,823 subjects, 3147 (24.5%) fulfilled the diagnostic criteria of NAFLD, and the prevalence in men and women was 28.8% and 16.3%, respectively. More information regarding the clinical data and related data process is available in Supplementary Material 2.

2.2.2. APOA1 Levels and Their Association with NAFLD. Fasting venous blood from the cubital vein and centrifuged was used to prepare the serum for biochemical analysis. The APOA1 levels were studied using the AU640 fully automatic biochemical analyzer (Olympus, Kobe, Japan). To explore the relationship between APOA1 levels and the prevalence of NAFLD, the 12,823 subjects were separated into four different groups according to their serum APOA1 levels, which were described as follows. (1) Q1 group: APOA1 level ≤ 1.18 g/L; (2) Q2 group: APOA1 level was between 1.19 and 1.32 g/L; (2) Q3 group: APOA1 level was between 1.33 and 1.55 g/L; and (2) Q4 group: APOA1 level ≥ 1.56 g/L in the Q4 group. A chi-square test was used to test the prevalence of NAFLD under different APOA1 levels. Multivariate logistic regression was used to analyze corisk factors of NAFLD besides APOA1 levels.

2.2.3. APOA1-Driven Signaling Pathway for NAFLD. Assisted by the literature-based Pathway Studio (http://www.pathwaystudio.com) knowledge database, we identified common genes and small molecules that were downstream targets of APOA1 and upstream regulators of NAFLD. These relation data were then used to compose the APOA1 seeded pathways, which was tentative to explore the possible mechanisms underlying the role of APOA1 in the pathology of NAFLD. A manual quality control process was conducted to ensure the reliability of the relationships and their polarities. A reference list was provided in Supplementary Material 1.

3. Result

3.1. PPAR-APOA1 Signaling Pathway for NAFLD. Literature-based pathway analysis showed that PPARs promote the synthesis and secretion of APOA1 in hepatocytes, as shown in Figure 1. The PPARD➔APOA1 relationship was supported by six independent studies; the PPARG➔APOA1 relationship was supported by 11 independent studies, and over 30 studies supported the PPARA➔APOA1 relationship. Regarding the association between APOA1 and NAFLD, on the one hand, two studies showed that modulation of APOA1 activity might have a beneficial effect on NASH, and the deficiency of APOA1 facilitates hepatic diet-induced deposition of triglycerides and NAFLD development in mice. On the other hand, multiple studies showed that serum APOA1 levels were significantly decreased in NAFLD patients. These previous studies support APOA1 as a vital hub protein within the PPAR pathway to play a beneficial role in the development of NAFLD.

Moreover, two drugs (fenofibrate and gemfibrozil) employed in NAFLD treatment were identified as promoters for all three PPARs, which also increase APOA1 mRNA in human liver biopsies as well as APOA1 plasma concentration. These studies extended the PPAR-APOA1 signaling pathway and provided further support for its role in NAFLD pathology. In total, over 1,200 references support the relationships presented in Figure 1, which is available at the worksheet of "Ref for PPARs-APOA1 pathway" in Supplementary Material 1.

3.2. Clinical Study Supporting APOA1–NAFLD Relationship. Due to the limited support from previous studies regarding the role of serum APOA1 in NAFLD, in this study, we employed large-scale clinical data to test the association between the variation of APOA1 levels and the prevalence of NAFLD. Our results indicated that the prevalence of NAFLD could decrease with elevated APOA1 levels, and that low serum APOA1 levels might be an independent risk factor for the prevalence of NAFLD.

3.2.1. Prevalence of NAFLD. NAFLD prevalence in Q1, Q2, Q3, and Q4 groups was 32.58%, 28.21%, 21.55%, and 15.58%, respectively. With the increase of APOA1 concentration, the prevalence of NAFLD was significantly decreased ($\chi^2 = 292.109$, $P < 0.001$), as shown in Table 1.

3.2.2. Multivariate Logistic Regression Analysis of Risk Factors of NAFLD. We explored the possibility of the decreased APOA1 levels as a risk for NAFLD incidence with/without adjusting other confounding factors and presented the results in Table 2. In the unadjusted model (model 1), compared with individuals in baseline serum APOA1 levels in group 1, the odds ratios (ORs) and 95% confidence intervals (CI) for NAFLD prevalence were 0.814 (0.731-.905), 0.568 (0.508-0.636), and 0.382 (0.339-0.431) for individuals in group 2, group 3, and group 4, respectively. With the increase of APOA1 levels (group 1 to group 4), the ORs for NAFLD prevalence were decreased, indicating the beneficial role of increased APOA1 levels in NAFLD.

When other risk factors were adjusted (model 2 and model 3), the ORs were increased, suggesting APOA1 as an independent risk factor for NAFLD. Especially in the group where APOA1 levels were high (group 3 and group

Table 2: MLR results of risk factors of NAFLD according to serum APOA1 quintiles.

APOA1 Quartile	n	Model 1		Model 2		Model 3	
		P value	OR (95% CI)	P value	OR(95% CI)	P value	OR (95% CI)
Q1	3300		1		1		1
Q2	3165	<0.000	0.814 (0.731-.905)	0.806	0.984 (0.869-1.115)	0.479	1.055 (0.913-.220)
Q3	3156	<0.000	0.568 (0.508-0.636)	0.002	0.812 (0.711-0.927)	0.005	0.790 (0.670-.932)
Q4	3202	<0.000	0.382 (0.339-0.431)	<.0001	0.625 (0.539-0.724)	<.0001	0.562 (0.452-.699)

Note: model 1 does not adjust for confounding factors; model 2 adjusted age, gender, and body mass index; model 3 adjusted age, sex, body mass index, waist circumference, uric acid, systolic blood pressure, diastolic blood pressure, total cholesterol, triacylglycerol, low-density lipoprotein cholesterol, high-density lipoprotein cholesterol, fasting blood glucose, alanine aminotransferase, aspartate aminotransferase, and glutamyltranspeptidase.

4), the influence of APOA1 levels was statistically significant in all models with/without adjusting other confounding factors. These results indicated that the increased serum APOA1 levels could be more critical than the deficiency of serum APOA1 in their influence on NAFLD development. Our results supported the APOA1–NAFLD relationship within the PPAR-APOA1 signaling pathway constructed in Figure 1.

3.3. APOA1 Seeded Signaling Pathway for NAFLD. Both literature-based pathway analysis and our clinical data suggested that increased APOA1 levels might play a beneficial role in NAFLD. To understand the underlying mechanisms, we conducted a literature-based molecule pathway analysis to identify downstream targets of APOA1 that were also upstream regulators of NAFLD, based on which APOA1-driven signaling pathways influencing NAFLD development were constructed and presented in Figure 2.

Overall, APOA1 beneficially regulated 16 out of 21 NAFLD regulators, highlighted in green-yellow or green-blue in Figures 2(a) and 2(b)). Specifically, APOA1 inhibited 10 NAFLD promoters (highlighted by green-yellow) and activated six NAFLD inhibitors (highlighted by green-blue), which might partially explain the beneficial role of APOA1 in the pathology of NAFLD. However, we also noted that increased APOA1 might promote five NAFLD promoters (highlighted in red), adding complexity to the APOA1-NAFLD relationship. The supporting references and the corresponding descriptive sentences for the relationships presented in Figures 2(a) and 2(b)) were provided in the worksheet of "Ref for APOA1 Molecule pathway" of Supplementary Material 1.

4. Discussion

All three peroxisome proliferator-activated receptors (PPARA, PPARD, and PPARG) attenuate NAFLD and thus were suggested as therapeutic targets for the treatment of NAFLD [5–7]. Results from a recent phase 2b clinical trial study showed that the pan-PPAR agonist lanifibranor could modulate key metabolic, inflammatory, and fibrogenic pathways in the pathogenesis of NASH, indicating the beneficial effect of the activation of PPARs on NAFLD [17]. However, the mechanism regarding PPAR-NAFLD regulation remains vague [8, 9]. Results from this study showed that APOA1 could be a hubprotein within the PPAR signaling pathway regulating the pathologic development of NAFLD.

Multiple previous studies supported the positive regulation of PPARs on APOA1. For instance, Gervois et al. showed that the PPARA activation could induce hepatic APOA1 and APOA2 expression in humans and lead to increased plasma HDL cholesterol [18]. Singh et al.'s study suggested that hepatic APOA1 and APOA2 expression could also be increased by the activation of PPARG [19]. In addition, PPARD has been reported to increase APOA1 and high-density lipoprotein synthesis through the activation of the ATP-binding cassette transporter 1 (ABCA1) gene [20]. These studies supported that APOA1 could be a common downstream target for all three PPARs.

Moreover, multiple studies supported the association between decreased levels of APOA1 and the prevalence of NAFLD [13, 20], and one study suggested a beneficial effect of increased APOA1 levels on NAFLD [15]. Results from our clinical data analysis confirmed that elevated serum APOA1 levels might function as an independent protective factor for the development of NAFLD (Tables 1 and 2). Taken together, these results suggested that increased APOA1 levels within the PPAR-APOA1 pathway could exert a beneficial role in protecting against the development of NAFLD.

Interestingly, literature-based pathway analysis also showed that PPARs (PPARA, PPARD, and PPARG), as well as APOA1, were downstream targets of two drugs (fenofibrate and gemfibrozil) that have the potential to be used in the treatment of NAFLD [21, 22], as shown in Figure 1. These results extended the PPAR-APOA1 signaling pathway and added support to its role in NAFLD.

As the mechanism of the APOA1-NAFLD relationship was largely unknown, we conducted another literature-based molecule pathway analysis. Our results showed that APOA1 could modulate 16 out of 21 NAFLD regulators in favor of a protective role against NAFLD development (Figure 2). For example, APOA1 could decrease the mRNA expression and production of IL1B [23], which plays a vital role in the pathologic development of NAFLD [24]. This built an APOA1–|IL1B–+>NAFLD pathway. Another example was the APOA1–+>ADIPOQ–|NAFLD pathway. APOA1 mimetic has been shown to induce the expression of ADIPOQ [25], which inhibits NAFLD by reducing fat content and promoting fatty acid oxidation [26]. For more of these pathways and their supporting references, please

refer to Figure 2 and the worksheet "Ref for APOA1 Molecule pathway" of Supplementary Material 1. These pathways might add new insights into the understanding of the role of APOA1 in the pathogenesis of NAFLD.

This study has one limitation as follows. The PPAR-APOA1 pathway was built mainly based on previous studies and partially on clinical data. Due to the complexity of the relationship between PPARs and NAFLD, the composed pathway in this study should be tested in a biology experiment.

5. Conclusions

This study integrated literature-based pathway analysis and clinical data analysis to study the PPAR-APOA1 signaling pathway and their role in the pathologic development of NAFLD. Our results showed that the three PPARs (PPARA, PPARD, and PPARG) might promote the expression and molecular transportation of APOA1, which mainly plays a beneficial role in the development of NAFLD. Our results may add new insights into the understanding of the role PPARs play in NAFLD.

Data Availability

All data generated or analyzed during this study are available upon request.

Conflicts of Interest

The authors declare that there is no conflict of interest regarding the publication of this article.

Acknowledgments

This project is partially supported by the National Key R&D Program of China (No. 2017YFC0908103), Ningbo Natural Science Foundation (grant number 2017A610276), and the Science and Technology Program for Agriculture and Social Development Program of Yinzhou, Ningbo, China (No. 2021AS0053).

Supplementary Materials

Supplementary 1. Supplementary Material 1 is a two-worksheet excel file described as follows. The worksheet "Ref for PPARs-APOA1 pathway" contains reference information supporting the PPAR-APOA1 pathway (Figure 1), including the type of the relationship, supporting references, and related sentences from the references where the relationship has been identified. The worksheet "Ref for APOA1 Molecule pathway" contains reference information supporting the genetic and molecule pathways (Figure 2), including the type of the relationship, supporting references, and related sentences from the references where the relationship has been identified.

Supplementary 2. Supplementary Material 2 presents more detailed information of the clinical data and related data process, including participant's exclusion rules, general information collection process, blood biochemical index tests process, hepatic ultrasound examination process, statistical analysis method description, and background clinical data of the patients.

References

[1] N. Chalasani, Z. Younossi, J. E. Lavine et al., "The diagnosis and management of nonalcoholic fatty liver disease: practice guidance from the American Association for the Study of Liver Diseases," *Hepatology*, vol. 67, no. 1, pp. 328–357, 2018.

[2] D. Iser and M. Ryan, "Fatty liver disease–a practical guide for GPs," *Australian Family Physician*, vol. 42, no. 7, pp. 444–447, 2013.

[3] V. W. Wong, W. K. Chan, S. Chitturi et al., "Asia-Pacific Working Party on Non-alcoholic Fatty Liver Disease guidelines 2017-Part 1: Definition, risk factors and assessment," *Journal of Gastroenterology and Hepatology*, vol. 33, no. 1, pp. 70–85, 2018.

[4] M. E. Rinella and A. J. Sanyal, "Management of NAFLD: a stage-based approach," *Nature Reviews. Gastroenterology & Hepatology*, vol. 13, no. 4, pp. 196–205, 2016.

[5] Y. Li, C. Wang, J. Lu et al., "PPAR δ inhibition protects against palmitic acid-LPS induced lipidosis and injury in cultured hepatocyte L02 cell," *International Journal of Medical Sciences*, vol. 16, no. 12, pp. 1593–1603, 2019.

[6] C. W. Wu, E. S. Chu, C. N. Lam et al., "PPARγ is essential for protection against nonalcoholic steatohepatitis," *Gene Therapy*, vol. 17, no. 6, pp. 790–798, 2010.

[7] Y. Jia, C. Wu, J. Kim, B. Kim, and S. J. Lee, "Astaxanthin reduces hepatic lipid accumulations in high-fat-fed C57BL/6J mice via activation of peroxisome proliferator-activated receptor (PPAR) alpha and inhibition of PPAR gamma and Akt," *The Journal of Nutritional Biochemistry*, vol. 28, pp. 9–18, 2016.

[8] L. Tong, L. Wang, S. Yao et al., "PPARδ attenuates hepatic steatosis through autophagy-mediated fatty acid oxidation," *Cell Death & Disease*, vol. 10, no. 3, p. 197, 2019.

[9] T. Lin, L. Li, C. Liang, and L. Peng, "Network pharmacology-based investigation of the therapeutic mechanisms of action of Danning tablets in nonalcoholic fatty liver disease," *Evidence-based Complementary and Alternative Medicine*, vol. 2021, 3495313 pages, 2021.

[10] E. P. C. van der Vorst, "High-density lipoproteins and apolipoprotein A1," *Sub-Cellular Biochemistry*, vol. 94, pp. 399–420, 2020.

[11] J. L. Breslow, D. Ross, J. McPherson et al., "Isolation and characterization of cDNA clones for human apolipoprotein A-I," *Proceedings of the National Academy of Sciences of the United States of America*, vol. 79, no. 22, pp. 6861–6865, 1982.

[12] K. C. Sung, M. C. Ryan, and A. M. Wilson, "The severity of nonalcoholic fatty liver disease is associated with increased cardiovascular risk in a large cohort of non-obese Asian subjects," *Atherosclerosis*, vol. 203, no. 2, pp. 581–586, 2009.

[13] S. H. PARK, B. I. KIM, J. W. YUN et al., "Insulin resistance and C-reactive protein as independent risk factors for non-alcoholic fatty liver disease in non-obese Asian men," *Journal of Gastroenterology and Hepatology*, vol. 19, no. 6, pp. 694–698, 2004.

[14] X. Y. Ren, D. Shi, J. Ding et al., "Total cholesterol to high-density lipoprotein cholesterol ratio is a significant predictor of nonalcoholic fatty liver: Jinchang cohort study," *Lipids in Health and Disease*, vol. 18, no. 1, p. 47, 2019.

[15] J. Mao, W. Liu, and Y. Wang, "Apolipoprotein A-I expression suppresses COX-2 expression by reducing reactive oxygen species in hepatocytes," *Biochemical and Biophysical Research Communications*, vol. 454, no. 3, pp. 359–363, 2014.

[16] M. K. Kim, Y. N. Chae, M. H. Son et al., "PAR-5359, a well-balanced PPARα/γ dual agonist, exhibits equivalent antidiabetic and hypolipidemic activities in vitro and in vivo," *European Journal of Pharmacology*, vol. 595, no. 1-3, pp. 119–125, 2008.

[17] S. M. Francque, P. Bedossa, V. Ratziu et al., "A randomized, controlled trial of the pan-PPAR agonist lanifibranor in NASH," *The New England Journal of Medicine*, vol. 385, no. 17, pp. 1547–1558, 2021.

[18] P. Gervois, I. P. Torra, J. C. Fruchart, and B. Staels, "Regulation of lipid and lipoprotein metabolism by PPAR activators," *Clinical Chemistry and Laboratory Medicine*, vol. 38, no. 1, pp. 3–11, 2000.

[19] V. Singh, R. Sharma, A. Kumar, and P. Deedwania, "Low high-density lipoprotein cholesterol: current status and future strategies for management," *Vascular Health and Risk Management*, vol. 6, pp. 979–996, 2010.

[20] J. Camps, J. Marsillach, A. Rull, C. Alonso-Villaverde, and J. Joven, "Interrelationships between paraoxonase-1 and monocyte chemoattractant protein-1 in the regulation of hepatic inflammation," *Advances in Experimental Medicine and Biology*, vol. 660, pp. 5–18, 2010.

[21] I. E. Triantaphyllidou, E. Kalyvioti, E. Karavia, I. Lilis, K. E. Kypreos, and D. J. Papachristou, "Perturbations in the HDL metabolic pathway predispose to the development of osteoarthritis in mice following long-term exposure to western-type diet," *Osteoarthritis and Cartilage*, vol. 21, no. 2, pp. 322–330, 2013.

[22] X. Z. Hong, L. D. Li, and L. M. Wu, "Effects of fenofibrate and Xuezhikang on high-fat diet-induced non-alcoholic fatty liver disease," *Clinical and Experimental Pharmacology & Physiology*, vol. 34, no. 1-2, pp. 27–35, 2007.

[23] M. Akcam, A. Boyaci, O. Pirgon, S. Kaya, S. Uysal, and B. N. Dundar, "Therapeutic effect of metformin and vitamin E versus prescriptive diet in obese adolescents with fatty liver," *International Journal for Vitamin and Nutrition Research*, vol. 81, no. 6, pp. 398–406, 2011.

[24] N. A. Ramella, I. Andújar, J. L. Ríos, S. A. Rosú, M. A. Tricerri, and G. R. Schinella, "Human apolipoprotein A-I Gly26Arg stimulation of inflammatory responses via NF-kB activation: potential roles in amyloidosis?," *Pathophysiology*, vol. 25, no. 4, pp. 397–404, 2018.

[25] S. Hua, M. Tara, W. Hua, and N. Hong-Min, "Necroptosis in ischemia-reperfusion injury of lean and steatotic livers," *Liver Research*, vol. 3, no. 3-4, pp. 227–233, 2019.

[26] J. S. Marino, S. J. Peterson, M. Li et al., "ApoA-1 mimetic restores adiponectin expression and insulin sensitivity independent of changes in body weight in female obese mice," *Nutrition & Diabetes*, vol. 2, no. 3, p. e33, 2012.

Hindawi
PPAR Research
Volume 2021, Article ID 7056506, 17 pages
https://doi.org/10.1155/2021/7056506

Research Article

Identification of a Novel PPAR Signature for Predicting Prognosis, Immune Microenvironment, and Chemotherapy Response in Bladder Cancer

Ke Zhu,[1] Wen Deng,[1] Hui Deng,[1] Xiaoqiang Liu,[1] Gongxian Wang,[1,2] and Bin Fu[1,2]

[1]*Department of Urology, The First Affiliated Hospital of Nanchang University, China*
[2]*Jiangxi Institute of Urology, Nanchang, Jiangxi 330006, China*

Correspondence should be addressed to Gongxian Wang; wanggx-mr@126.com and Bin Fu; urofubin@sina.com

Received 27 October 2021; Revised 10 December 2021; Accepted 13 December 2021; Published 30 December 2021

Academic Editor: Hongbao Cao

Background. Mounting evidence has confirmed that peroxisome proliferator-activated receptors (PPARs) played a crucial role in the development and progression of bladder cancer (BLCA). The purpose of this study is to comprehensively investigate the function and prognostic value of PPAR-targeted genes in BLCA. *Methods.* The RNA sequencing data and clinical information of BLCA patients were acquired from The Cancer Genome Atlas (TCGA). The differentially expressed PPAR-targeted genes were investigated. Cox analysis and least absolute shrinkage and selection operator (LASSO) analysis were performed for screening prognostic PPAR-targeted genes and constructing the prognostic PPAR signature and then validated by GSE13507 cohort and GSE32894 cohort. A nomogram was constructed to predict the outcomes of BLCA patients in combination with PPAR signature and clinical factors. Gene set enrichment analysis (GSEA) and immune cell infiltration were implemented to explore the molecular characteristics of the signature. The Genomics of Drug Sensitivity in Cancer (GDSC) database was used to predict the chemotherapy responses of the prognostic signature. The candidate small molecule drugs targeting PPAR-targeted genes were screened by the CMAP database. *Results.* We constructed and validated the prognostic signature comprising of 4 PPAR-targeted genes (CPT1B, CALR, AHNAK, and FADS2), which was an independent prognostic biomarker in BLCA patients. A nomogram based on the signature and clinical factors was established in the TCGA set, and the calibration plots displayed the excellent predictive capacity. GSEA analysis indicated that PPAR signature was implicated in multiple oncogenic signaling pathways and correlated with tumor immune cell infiltration. Patients in the high-risk groups showed greater sensitivity to chemotherapy than those in the low-risk groups. Moreover, 11 candidate small molecule drugs were identified for the treatment of BLCA. *Conclusion.* We constructed and validated a novel PPAR signature, which showed the excellent performance in predicting prognosis and chemotherapy sensitivity of BLCA patients.

1. Introduction

Bladder cancer (BLCA) is one of the common causes of cancer-related deaths with elevated heterogeneity, accounting for over 200,000 cancer-related deaths in 2020 [1]. According to the tumor with or without muscle invasion, BLCA is classified into non-muscle-invasive BLCA (NMIBLCA) and muscle-invasive BLCA (MIBLCA). The former is characterized by recurrence and progression while the latter is characterized by metastasis and unfavorable prognosis [2]. Despite the uplifting improvement in cancer therapy for the past two decades, including laparoscopic and robotic surgery, targeted therapy, and immune checkpoint inhibitor therapy, the 5-year survival rate of patients with MIBLCA remains unsatisfactory. Therefore, identifying novel biomarkers for predicting prognosis and response to therapeutic drug in BLCA is of considerable clinical meaning.

Peroxisome proliferator-activated receptors (PPARs) were the critical members of the steroid hormone receptor family. Meanwhile, PPARs were also a group of specific nuclear transcription factors activated by natural ligands (fatty acids and eicosanoids) and synthetic ligands (fibrates

and thiazolidinediones) [3]. According to the various tissue distribution, metabolic patterns, and ligand specificity, PPARs were classified into three isotypes: PPARα, PPARβ/δ, and PPARγ [4]. PPARα was mainly located in brown adipose tissue and liver and involved in eliminating cellular or circulating lipids [5, 6]. PPARγ was primarily expressed in the adipose tissue and the immune system and correlated with adipose differentiation. PPARβ/δ was highest expressed in the gut, kidney, and heart and mainly implicated in lipid oxidation and cell proliferation. Accumulating studies have certified the crucial roles of PPARs in various biological processes including cell differentiation, apoptosis, inflammation, immune function, angiogenesis, metabolism, and carcinogenesis [3, 7–10]. Furthermore, several drugs that targeted PPARs have been applied in clinical trials [11]. However, the relationship between PPARs and outcomes of BLCA patients was still unknown.

In the present study, we investigated the expression and outcomes of PPARs through integrated bioinformatic approaches in BLCA. Subsequently, a PPAR-based signature was established for predicting the prognosis and drug sensitivity, and the predictive ability of this signature was validated in two external datasets. Furthermore, we also explored the correlation between the signature and clinical characteristics as well as tumor microenvironment. In addition, enrichment analysis was conducted to investigate the potential mechanisms of PPARs in BLCA. Finally, a nomogram was constructed to improve the clinical management of BLCA patients.

2. Materials and Methods

2.1. Data Acquisition. The RNA-sequencing data and clinical characteristic information of patients with BLCA were acquired from The Cancer Genome Atlas database (TCGA, https://gdc-portal.nci.nih.gov/). In addition, GSE13507 and GSE32894 were originated from the Gene Expression Omnibus database (GEO, https://www.ncbi.nlm.nih.gov/geo/) and served as the independent external validation datasets. 130 experimentally verified PPAR-targeted genes were obtained from the PPARgene database (http://www.ppargene.org/) [12].

2.2. Identification of Differentially Expressed PPAR Genes. The differential expression analysis was conducted with the edgeR package in R software (version R 3.6.1). Differentially expressed PPAR genes (DEPPARGs) were identified with the criterion of false discovery rate (FDR) < 0.05 and |log 2 FC (fold change) | >1 between BLCA and normal samples. Heatmap and volcano plot were used to display DEPPARGs. In addition, Gene Ontology (GO) analysis and Kyoto Encyclopedia of Genes and Genomes (KEGG) analysis were performed to investigate the potential functions of DEPPARGs by using the clusterProfiler packages in R software.

2.3. Identification of Candidate Small Molecule Drugs. To identify the potential small molecule drugs for treatments of patients with BLCA, the Connectivity Map database (CMAP, https://portals.broadinstitute.org/cmap/) was performed to select the candidate drugs. The enrichment score was used to evaluate the effect of a drug, and the negative score indicated that a drug might have antitumor activity.

2.4. Establishment and Validation of the PPAR-Related Prognostic Signature. To identify the DEPPARGs associated with overall survival (OS), univariate Cox regression analysis was performed to explore the relationship between DEPPARGs and prognosis of BLCA patients in the TCGA dataset. All the DEPPARGs with P value < 0.05 were identified as candidate genes for subsequent analyses. Then, the least absolute shrinkage and selection operator (LASSO) analysis was used to shun the overfitting and identify optimal prognostic DEPPARGs. Finally, multivariate Cox regression analysis was conducted to establish an optimized risk score (PPARscore). The PPARscore of patients with BLCA was calculated by the following formula: $\text{PPARscore} = \sum_i^n X_i \times Y_i$ (where Y represented the mRNA expression of gene and X represented the coefficient of the relevant gene from the multivariate Cox analysis). Patients were classified into high- and low-risk groups based on the median risk score. Survival analyses were conducted to evaluate the difference of prognosis among different groups by R packages (survival and survminer) in R. In addition, a receiver operating characteristic (ROC) curve was performed to test the predictive performance of the signature by using the survivalROC package. Moreover, principal component analysis (PCA) and t-distributed stochastic neighbor embedding (t-SNE) were executed to investigate the distribution characteristics of patients among two groups. In addition, the predictive power of our constructed signature was verified in the two external validation datasets (GSE13507 and GSE32894) by using the same approach.

2.5. Gene Set Enrichment Analysis and Immune Infiltration Analyses. Gene set enrichment analysis (GSEA) was used to explore the underlying biological mechanisms of the PPAR-based signature with the criterion of P value < 0.05 and FDR < 0.25. Given the importance of the tumor immune microenvironment, the ESTIMATE algorithm was conducted to evaluate the stromal score, ESTIMATE score, and immune score among two groups. In addition, the CIBERSORT algorithm was performed to explore the immune cell infiltration levels of 22 distinct leukocyte subsets among different groups. Furthermore, we also investigated the correlation between PPARscore and key immune checkpoints (PD-1, PD-L1, CTLA4, LAG3, HAVCR2, and TIGIT). P values < 0.05 were considered as statistical criteria.

2.6. Chemotherapy Sensitivity Prediction. To assess the difference of chemotherapy sensitivity between different groups, we used the GDSC database to estimate the half-maximal inhibitory concentration (IC50) of chemotherapy drugs for predicting the sensitivity of chemotherapy drugs by using the package (pRRophetic). P values < 0.05 were considered statistically significant.

2.7. Construction of a Nomogram. Univariate and multivariate cox regression analyses were conducted to investigate whether the PPAR-based signature was an independent prognosis factor in patients with BLCA. Furthermore, we

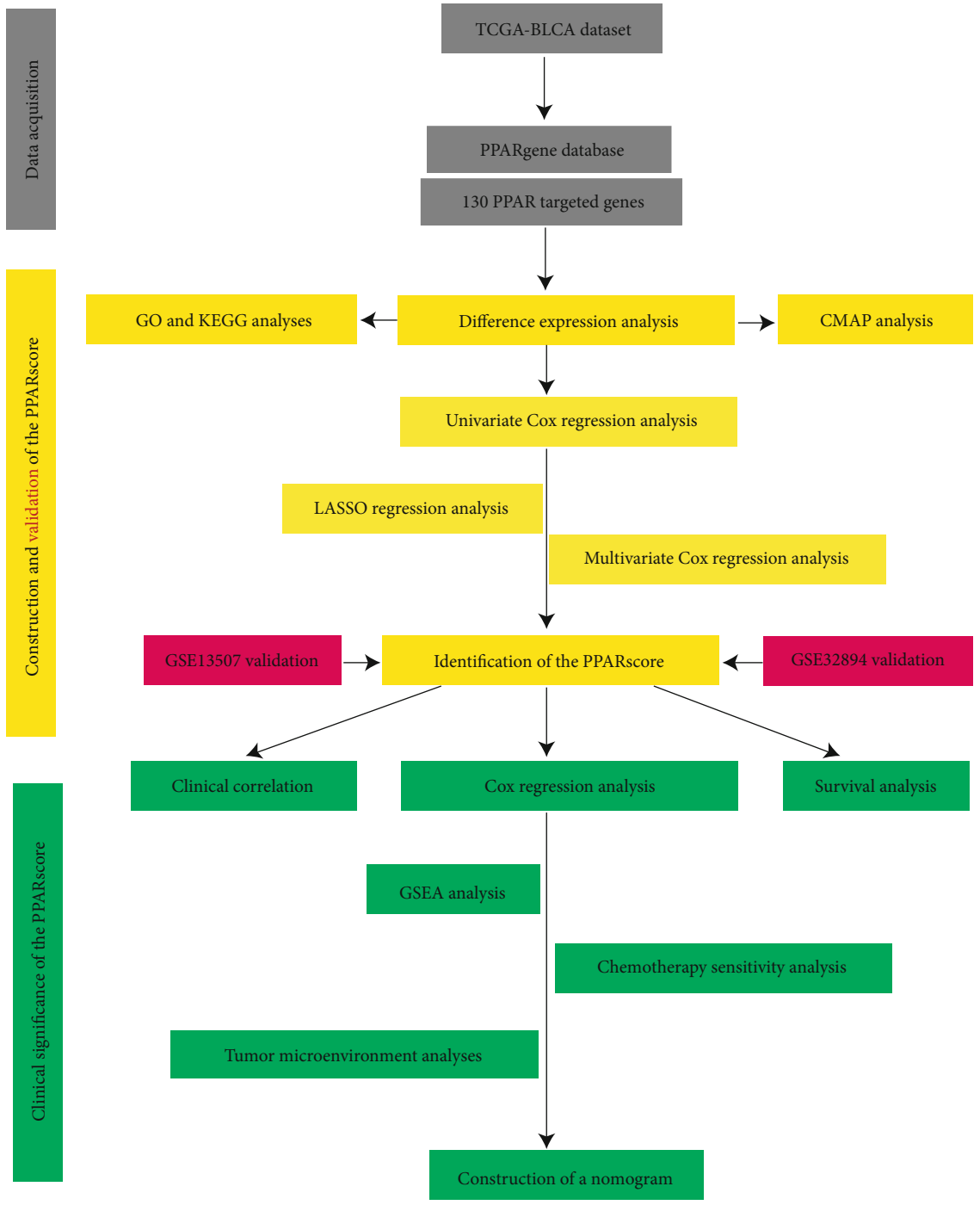

Figure 1: The flow chart of the PPAR signature in predicting survival of BLCA.

also categorized patients into various subgroups stratified by clinical features, and the Kaplan-Meier curves were conducted in each subgroup to further test the predictive power of the PPAR-based signature in predicting prognosis. Based on the results of multivariate analysis, a nomogram consisting of risk score and several clinical features for predicting the over survival of 3 and 5 years was established. The calibration curve was used to evaluate the accuracy of survival prediction in the nomogram.

3. Results

3.1. Identification of Differentially Expressed Genes. Figure 1 displays the procedure of our study. The mRNA expression profile of 130 PPAR target genes between BLCA samples ($n = 414$) and normal bladder samples ($n = 19$) was obtained from the TCGA dataset. A total of 27 DEPPARGs were identified with the threshold of FDR < 0.05 and $|\log 2\,FC| > 1$, including 15 downregulated and 12 upregulated genes

(Figure 2). The volcano map was used to exhibit the expression profile of DEPPARGs. To further expound the potential mechanisms of DEPPARGs, GO and KEGG analyses were performed with the 27 DEPPARGs. GO analysis indicated that DEPPARGs were mainly implicated in the regulation of lipid metabolic process, triglyceride metabolic process, acylglycerol metabolic process, neutral lipid metabolic process, lipid localization, and reactive oxygen species metabolic process (Supplementary Figure 1(a)). The result of KEGG analysis revealed that DEPPARGs were mainly involved in the PPAR signaling pathway, cholesterol metabolism, ovarian steroidogenesis, platinum drug resistance, and microRNAs in cancer (Supplementary Figure 1(b)), which suggested that DEPPARGs might function as the crucial role in the tumorigenesis, progression, and drug resistance of BLCA.

3.2. Small Molecular Drugs. To further enhance the therapeutic efficacy of BLCA, the CMAP database was performed to identify candidate drugs based on the DEPPARGs. The eleven small molecular drugs with anticancer activity were identified (Table 1). These drugs (vorinostat, cinchonine, helveticoside, lanatoside C, tiapride, idoxuridine, niclosamide, ampicillin, epitiostanol, pyrimethamine, and cephaeline) might alleviate the progression of BLCA and serve as novel potential targeted drugs for BLCA treatment.

3.3. Construction of a Prognostic PPAR Signature. Based on the 27 DEPPARGs, Cox and LASSO regression analyses were implemented to identify DEPPARGs correlated with OS in the TCGA dataset. First, ten DEPPARGs exhibited fairly correlation with the outcomes of patients with BLCA via univariate Cox regression analysis (Figure 3(a)). Then, to guarantee the reliability of ten prognostic genes, LASSO regression analysis was performed to further screen DEPPARGs without the overfitting (Figures 3(b) and 3(c)). Finally, based on the result of multivariate Cox regression analysis, four DEPPARGs, including CALR, FADS2, CPT1B, and AHNAK, were identified and applied to establish a prognostic signature (Figure 3(d)). We developed a four gene-based PPARscore as follows: PPARscore = (0.2739 × CALR expression) + (0.352 × AHNAK expression) + (−0.3324× CPT 1B expression) + (0.164 × FADS2 expression). Patients were then categorized into high- and low-risk groups in accordance with the median PPARscore. PCA and *t*-SNE analyses also displayed the various dimensions between the high-risk group and the low-risk group (Supplementary Figures 2(a) and 2(b)). The prognosis of patients in the low-risk group was significantly superior to those in the high-risk group ($P < 0.05$) (Figure 4(a)). Time-dependent ROC analysis suggested that the AUC values for 1-, 3-, and 5-year survival of PPARscore in the TCGA dataset were 0.647, 0.688, and 0.694, respectively (Figure 4(b)). These results indicated that the PPAR signature might have a certain applicability in predicting the outcomes of patients with BLCA. Additionally, the heatmap of the expression profiles of four genes showed that CALR, AHNAK, and FADS2 were highly expressed in the high-risk group, while CPT1B was elevated in the low-risk group (Figure 4(c)).

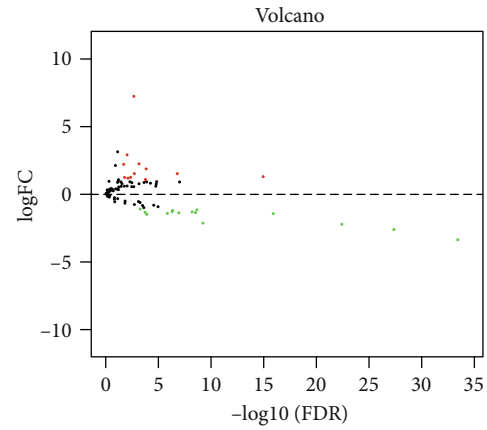

Figure 2: Volcano map showed the differentially expressed PPAR-targeted genes (DEPPARGs). The red plots represented the upregulated genes, the blue plots represented the underregulated genes, and the black plots represented no statistically differentially expressed genes with the criterion of FDR < 0.05 and |log 2 FC | > 1. FDR: false discovery rate; FC: fold change.

Table 1: The 11 small-molecule drugs of CMP database analysis.

cmap name	Mean	*n*	Enrichment	*P* value	Percent nonnull
Vorinostat	-0.766	2	-0.995	0.00008	100
Cinchonine	-0.697	2	-0.983	0.00058	100
Helveticoside	-0.83	2	-0.982	0.0007	100
Lanatoside C	-0.818	2	-0.981	0.00082	100
Idoxuridine	-0.64	2	-0.963	0.00304	100
Niclosamide	-0.621	2	-0.959	0.00368	100
Ampicillin	-0.607	2	-0.958	0.0038	100
Epitiostanol	-0.595	2	-0.952	0.00497	100
Tiapride	-0.652	2	-0.972	0.00159	100
Pyrimethamine	-0.57	2	-0.935	0.00891	100
Cephaeline	-0.521	2	-0.879	0.00347	100

3.4. Validation of the PPAR Signature. In GSE13507, survival time and status from 165 patients with BLCA were applied to validate our constructed signature. The PPARscore of each patient was generated with the same approach as before, and patients were classified into high- and low-risk groups in accordance with the median PPARscore. PCA and *t*-SNE analyses displayed the diverse dimensions between the high-risk group and the low-risk group (Supplementary Figures 2(c) and 2(d)). *K-M* curve analysis indicated that the prognosis of patients in the low-risk group was significantly superior to those in the high-risk group ($P < 0.05$) (Figure 5(a)). Time-dependent ROC analysis suggested that the AUC values for 1-, 3-, and 5-year survival of PPARscore in the TCGA dataset were 0.630, 0.672, and 0.671, respectively (Figure 5(b)). Similarly, in GSE32894, 224 patients containing survival time and status were served as another external validation dataset. The results of GSE32894 were also consistent with

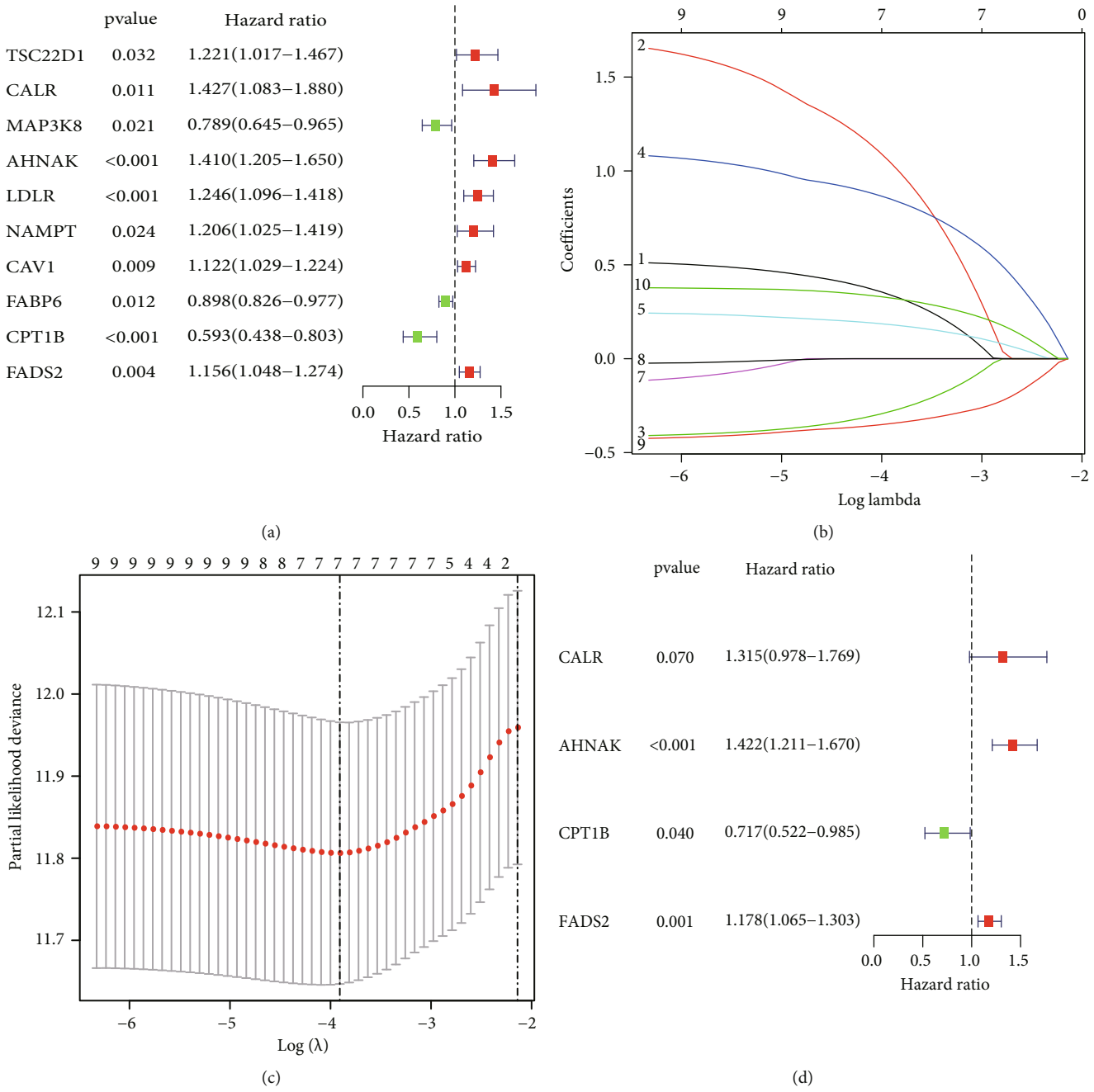

Figure 3: Identification of DEPPARGs correlated with prognosis in the TCGA dataset. (a) Identification of the prognostic DEPPARGs by univariate Cox regression analysis; (b) the coefficient profile of 9 prognostic genes by LASSO regression analysis; (c) tenfold cross-validation for tuning parameter selection in the LASSO analysis; (d) identification of 4 prognostic DEPPARGs by multivariate Cox regression analysis.

the previous results (Figures 5(e) and 5(f)). Taken together, all these results revealed that the PPAR signature might serve as a potential biomarker for predicting the outcomes of BLCA patients.

3.5. GSEA. To further illustrate the molecular mechanisms of PPAR signature, GSEA analysis was conducted. The results of GSEA analysis indicated that focal adhesion, pathways in cancer, GAP junction, chemokine signaling pathway, WNT signaling pathway, TGF-β signaling pathway, steroid biosynthesis, bladder cancer, MAPK signaling pathway, and calcium signaling pathway were mainly enriched in the high-risk group, suggesting that patients of high-risk groups were notably related to cancer-related signaling pathway, while oxidative phosphorylation and cardiac muscle contraction were highly enriched in the low-risk group (Supplementary Figure 3).

3.6. Immune Landscape of the PPAR Signature. To explore whether PPAR signature could illustrate the characteristic of tumor immune microenvironment, ESTIMATE and CIBERSORT algorithms associated with immune cell

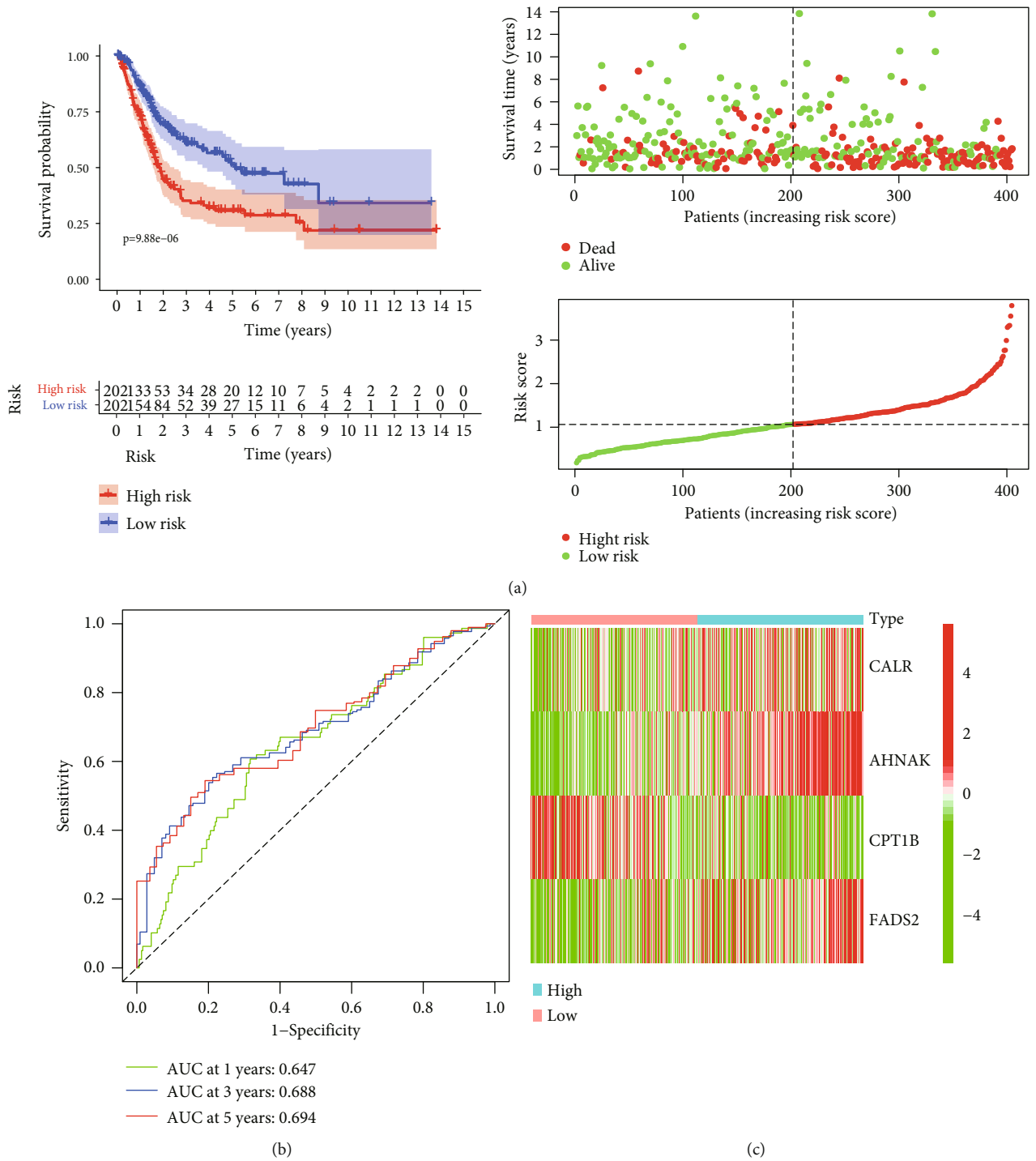

Figure 4: Construction of the PPAR signature correlated with prognosis in the TCGA dataset. (a) Kaplan-Meier curve showed that low-risk patients had better survival compared with the high-risk patients. The distribution of overall survival between the high-risk group and the low-risk group. The distribution of PPARscore between the high-risk group and the low-risk group; (b) time-independent receiver operating characteristic (ROC) analysis for evaluating the predictive performance of PPARscore; (c) heatmap showed the expression patterns of 4 genes between the high- and low-risk groups.

infiltration were conducted. The results of ESTIMATE suggested that patients with high PPARscore displayed a higher immune score, stromal score, and ESTIMATE score than patients with low PPARscore (Figure 6(a)), which indicated that PPARscore might be correlated with the tumor microenvironment. Furthermore, the results of CIBERSORT revealed that the proportions of CD8+ T cell, Tregs, plasma cell, and T cells gamma delta were obviously higher in patients with low PPARscore, while the proportions of M2 macrophages and M0 macrophages were remarkably higher

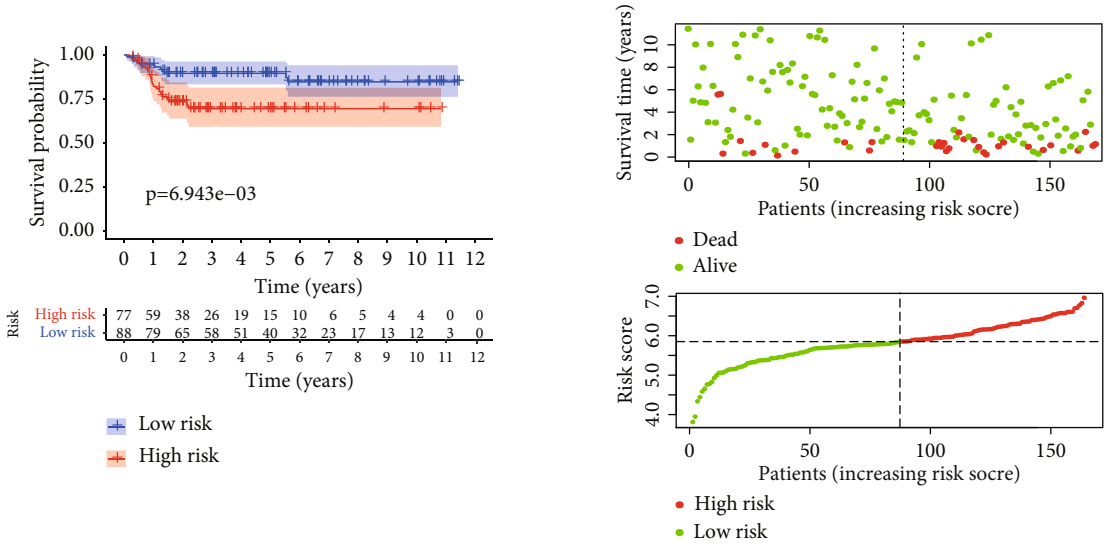

(a)

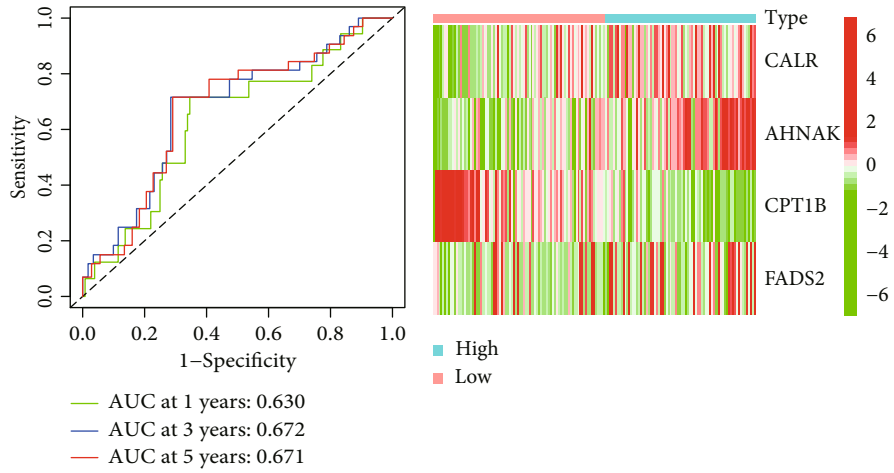

(b) (c)

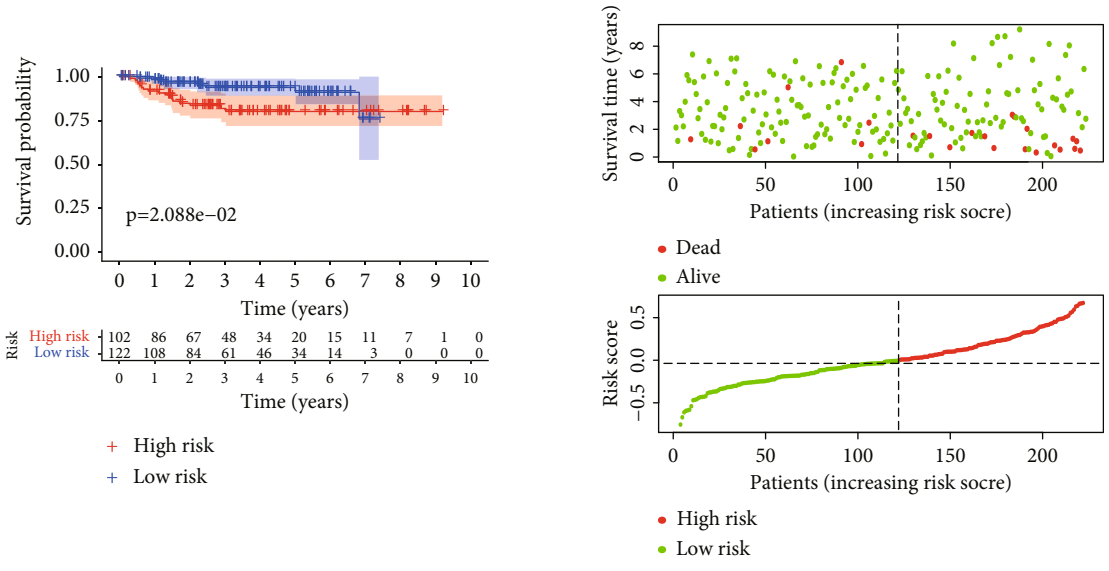

(d)

Figure 5: Continued.

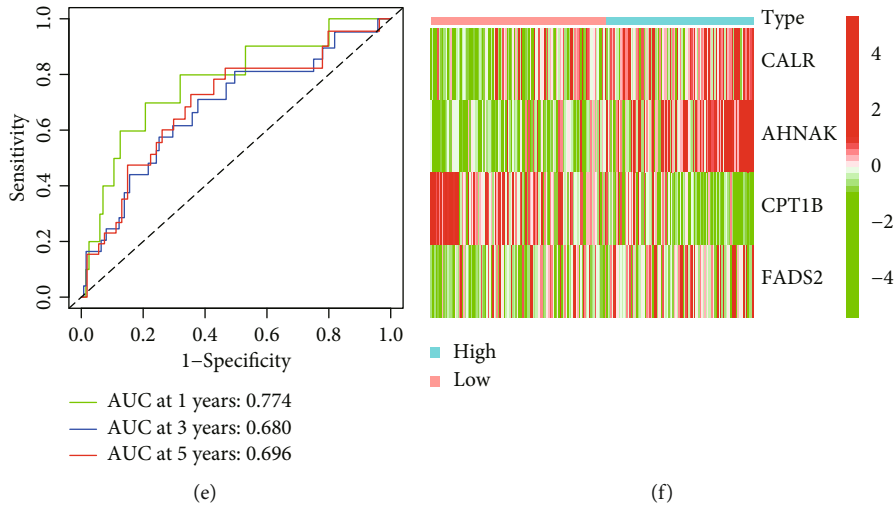

Figure 5: Validation of the PPAR signature in the GEO dataset. (a–e) Kaplan-Meier curve showed that low-risk patients had better survival compared with the high-risk patients. The distribution of overall survival between the high-risk group and the low-risk group. The distribution of PPARscore between the high-risk group and the low-risk group ((a) GSE13507; (e) GSE32894); (b–f) time-independent receiver operating characteristic (ROC) analysis for evaluating the predictive performance of PPARscore ((b) GSE13507; (f) GSE32894); (c–g) heatmap showed the expression patterns of 4 genes between the high- and low-risk groups ((c) GSE13507; (g) GSE32894). The blue box represented the GSE13507 dataset; the red box represented the GSE32894 dataset.

in patients with high PPARscore (Figure 6(b) and Supplementary Figure 4). In addition, we also compared the expression of key immune checkpoints between two groups and found that immune checkpoints (PD-L1, LAG3, TIGIT, and HAVCR2) were upregulated in the high-risk group, while the expressions of CTLA4 and PD-1 were no different among two groups (Supplementary Figure 5). All these results uncovered that the PPAR signature might be implicated in the tumorigenesis and progression of BLCA via regulating the infiltrating distribution of immune cells.

3.7. Chemotherapeutic Response Analysis. To improve the therapeutic effect of BLCA patients, we further investigated whether our PPAR signature could predict the sensitivity to several common chemotherapy drugs between two groups. The results of GDSC database analysis suggested that IC50 values of chemotherapy drugs including Bleomycin, Mitomycin C, Gemcitabine, Cyclopamine, Docetaxel, Cisplatin, Thapsignargin, Paclitaxel, Rapamycin, Parthenolide, Vinblastine, and Doxorubicin were elevated in patients with low PPARscore compared to those with high PPARscore, which indicated that patients with high PPARscore were much more sensitive to these chemotherapy drugs (Figure 7).

3.8. Relationship between PPAR Signature and Clinical Characteristics. To improve the clinical management of BLCA patients, we also explored the correlation between PPARscore and clinical characteristics in the TCGA dataset. Heatmap displayed the distributions of clinical characteristics including tumor grade, tumor stage, gender, age, N stage, and T stage between two groups, and obvious differences were observed in tumor grade, tumor stage, T stage, and N stage (Figure 8(a)). In addition, the boxplot exhibited the significant correlation between PPARscore with the poorer clinical characteristics (T3-T4 stage, N1-N2-N3 stage, stage III–IV, and grade high) (Figure 8(b)). These results suggested that PPARscore might be related to the progression of BLCA.

3.9. Construction of a Nomogram. Univariable and multivariable Cox analyses were applied to further explore whether PPARscore could be an independent prognostic indicator for BLCA patients. The result of univariable Cox analysis indicated that PPARscore, tumor stage, tumor grade, T stage, and N stage were obviously correlated with outcomes of BLCA patients (Figure 9(a)). The result of multivariable Cox analysis showed that PPARscore and age were still associated with outcomes of BLCA patients, which suggested that the PPARscore model could be an independent prognostic factor of BLCA patients (Figure 9(b)). Furthermore, multiparameter ROC curve analyses showed that the AUC value of PPARscore was 0.694 (Figure 9(c)), which suggested that PPARscore was superior to traditional clinical prognostic indicators in predicting outcomes. In addition, the results of subgroup analyses stratified by various clinical characteristics indicated an obviously shorter survival probability in patients with high PPARscore among various clinical characteristics except T1-T2 stage, and stage I-II subgroups (Supplementary Figure 6). Based on the result of multivariable Cox analysis, PPARscore and age were incorporated to construct a nomogram to preferably predict the survival ability of 3 and 5 years (Figure 10(a)). The calibration curves suggested that the nomogram exhibited the well performance in forecasting the prognosis (Figures 10(b) and 10(c)).

4. Discussion

In the current study, the expression pattern of PPAR-targeted genes could predict the outcomes of in BLCA, and

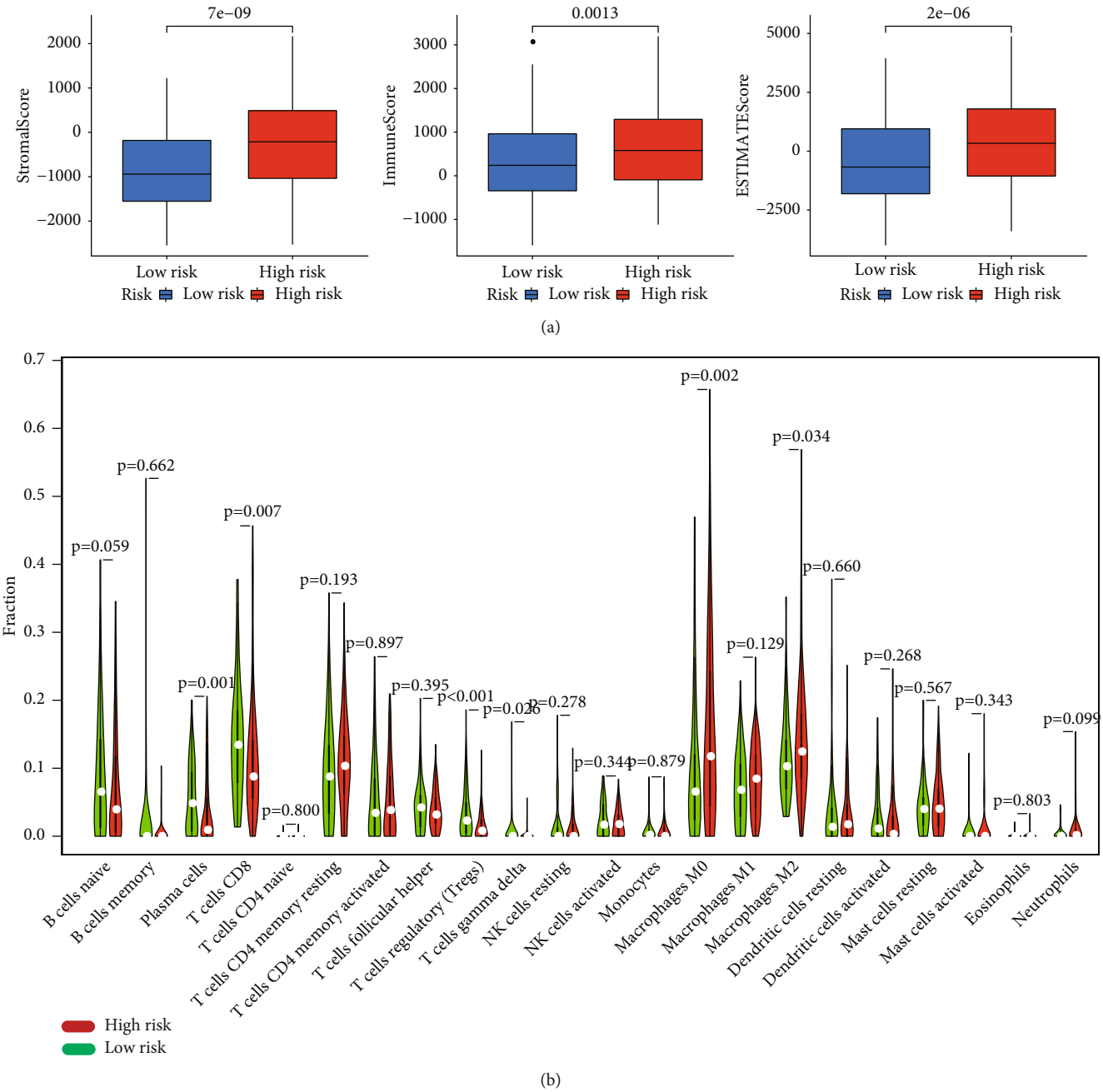

Figure 6: The relationship between PPARscore and tumor microenvironment. (a) Boxplot showed the relative expressions of ESTIMATE score, immune score, and stromal score between high- and low-risk groups by the ESTIMATE algorithm; (b) violin plot compared the expressions of 22 immune cells infiltrating between the high- and low-risk groups by the CIBERSORT algorithm. The red signified the high-risk groups, and the blue signified the low-risk groups.

four genes were applied to further construct and validate a prognostic PPARscore. Furthermore, PPARscore was also available in predicting sensitivity to chemotherapy drugs. In addition, PPARscore was also correlated with adverse clinical features and immune cells. In GSEA analysis, PPARscore was observed to be implicated in various signaling pathways correlated with tumorigenesis.

Four genes were incorporated in our signature (CPT1B, CALR, FADS2, and AHNAK). Carnitine palmitoyltransferase 1B (CPT1B), a crucial enzyme of long-chain fatty acid β-oxidation and also a member of the PPAR pathway, has been found to be underexpressed in high-grade BLCA. In addition, the overexpression of CPT1B could inhibit the proliferation and metastasis of BLCA cells by accelerating fatty acid metabolism and reducing epithelial-mesenchymal transition (EMT) [13]. Calreticulin (CALR), a crucial member of endoplasmic reticulum (ER) chaperones, was positively related to superior prognosis owing to the

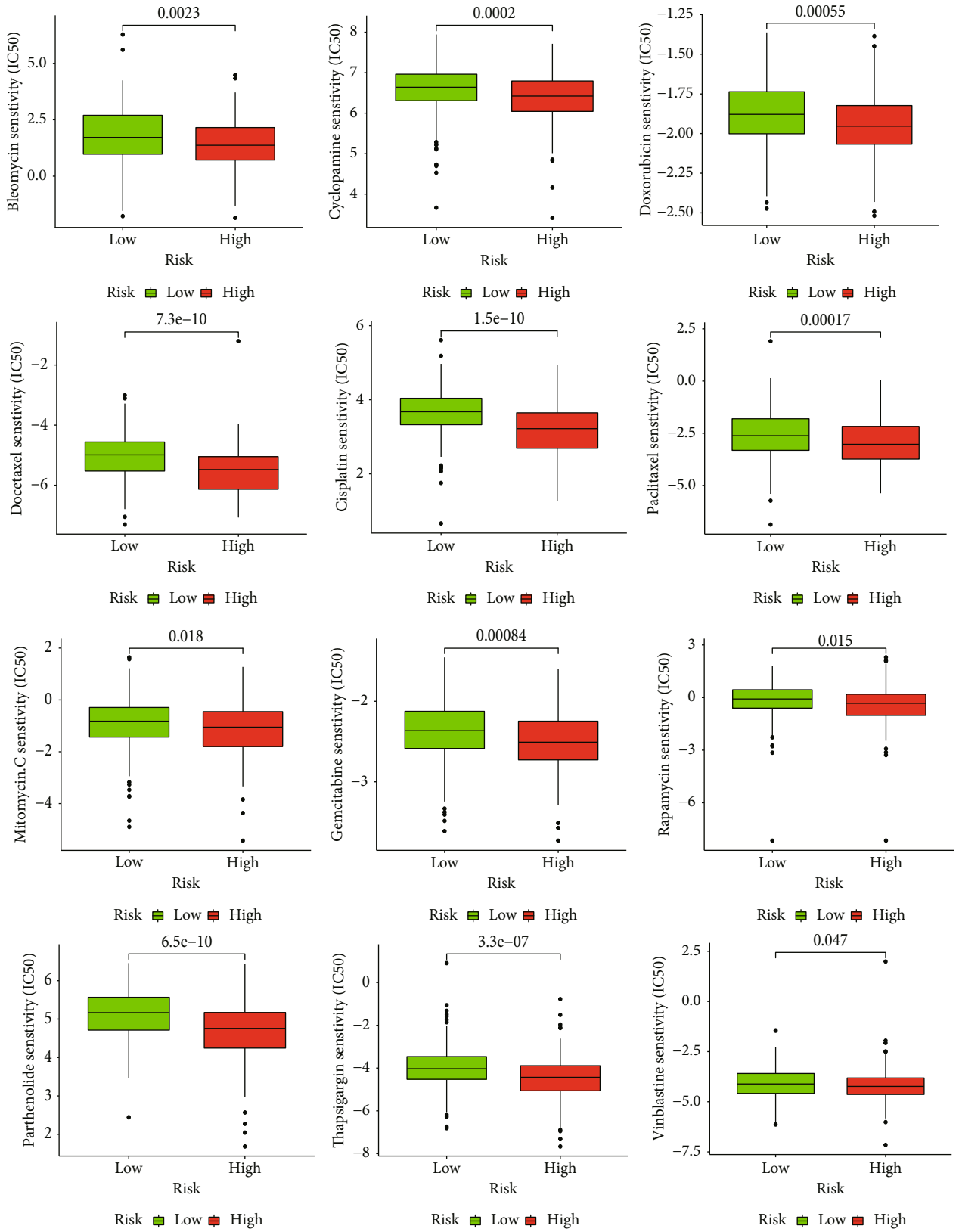

Figure 7: Comparison of the estimated IC50 values of Bleomycin, Mitomycin C, Gemcitabine, Cyclopamine, Docetaxel, Cisplatin, Paclitaxel, Rapamycin, Parthenolide, Thapsignargin, Vinblastine, and Doxorubicin in the high- and low-risk BLCA samples by using the GDSC database.

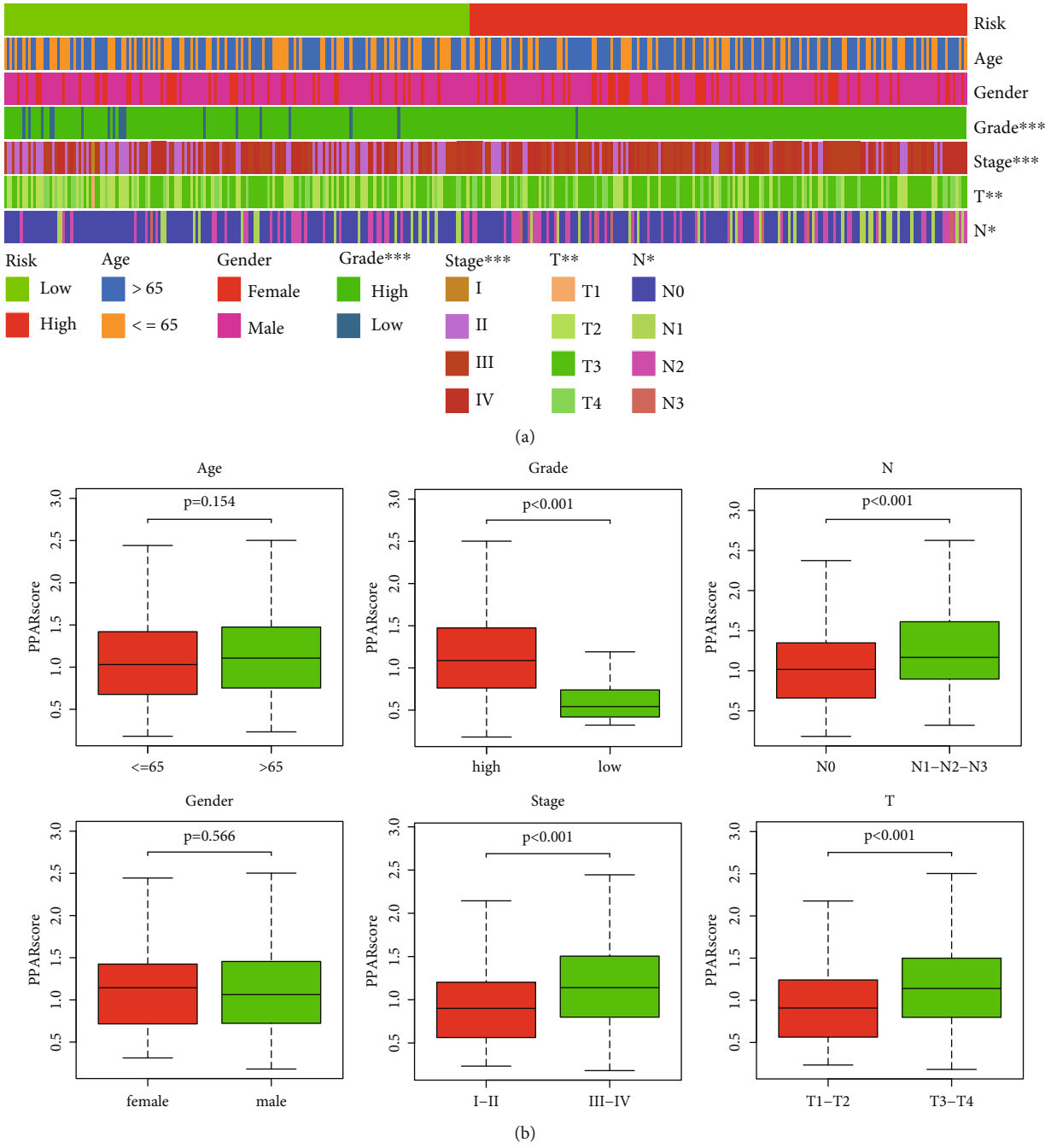

Figure 8: The correlation between the risk scores and clinicopathological factors. (a) Heatmap showed the relative expression of the risk score in BLCA patients at various clinical features, including age, gender, tumor grade, TNM stage, T stage, and N stage. $^{***}P < 0.001$ $<^{**}P < 0.01<^{*}P < 0.05$; (b) boxplot showed the relative expression of the risk score in BLCA patients at subgroups stratified by age, gender, tumor grade, TNM stage, T stage, and N stage.

activation of anticancer immune in various cancers [14–17]. CALR overexpression was obviously related to advanced grade and poor prognosis in BLCA [18, 19]. Fatty acid desaturase 2 (FADS2), a key enzyme of polyunsaturated fatty acid (PUFA) metabolism, was involved in multiple diseases including cancer. FADS2 was adversely related to prognosis in BLCA by bioinformatic analysis [20]. In addition, Jiang et al. also reported that FADS2 might serve as a ferroptosis suppressor [21]. The aberrant expression of AHNAK has been reported in various cancer [22–26]. For example, AHNAK overexpression inhibited the TNBC cell proliferation and lung metastasis by partly regulating the Wnt/β-catenin signaling pathway.

Subsequently, we performed GSEA analysis to further disclose the mechanism of PPAR signature in BLCA. The results confirmed that PPAR signature was involved in

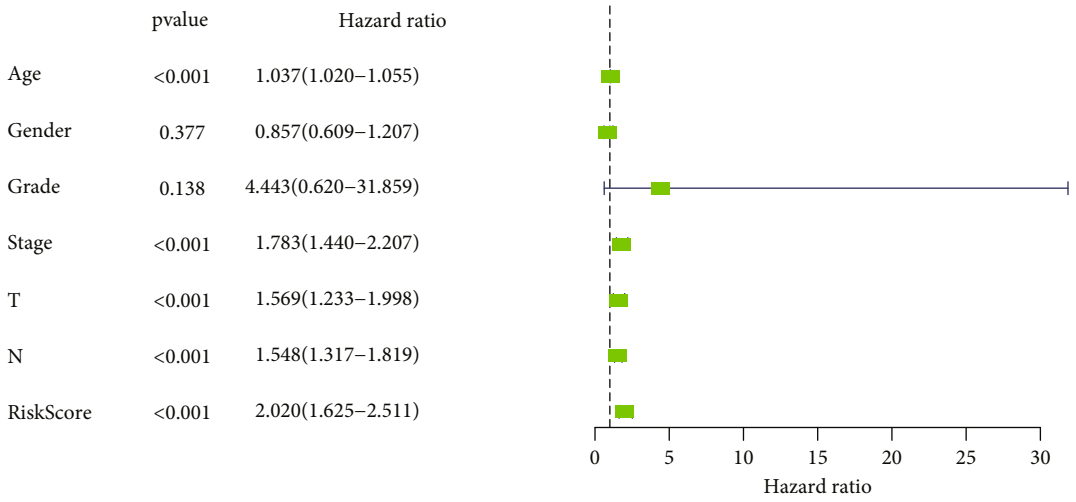

(a)

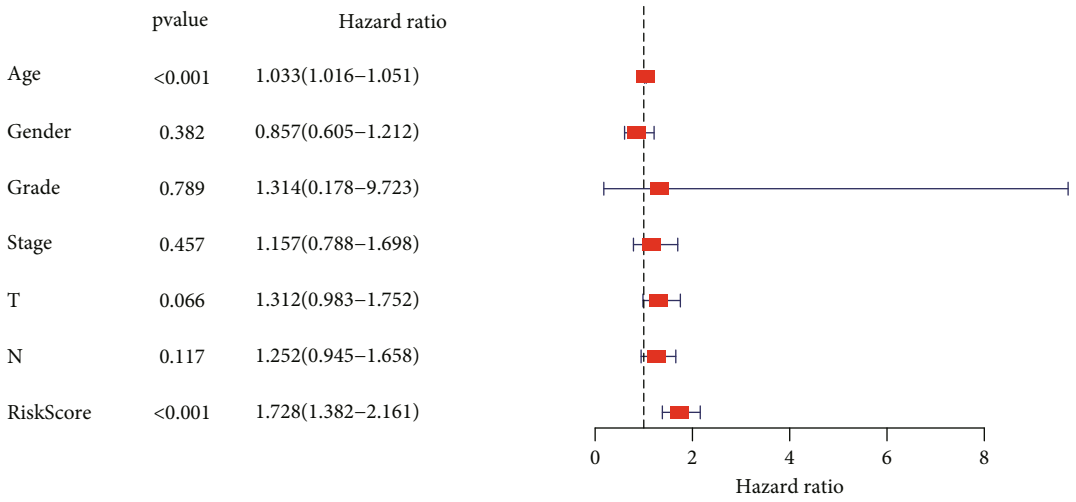

(b)

Figure 9: Continued.

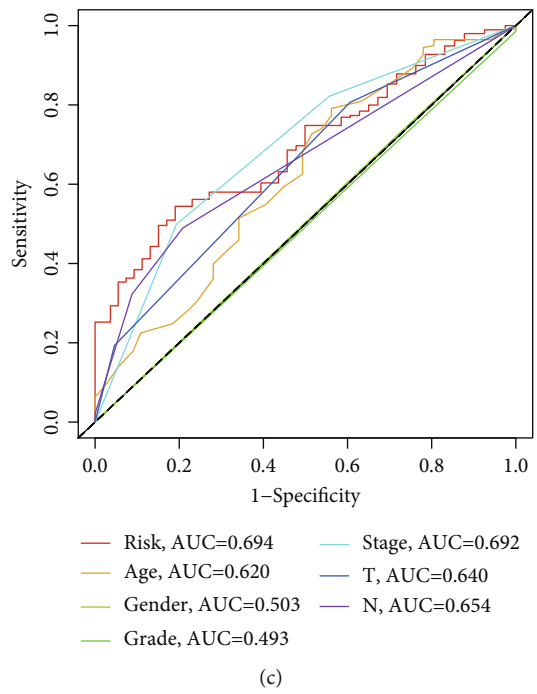

(c)

Figure 9: The PPAR signature was an independent prognostic factor for BLCA in the TCGA set. (a) The univariate Cox analysis for evaluating the independent prognostic value of PPAR signature; (b) multivariate Cox analysis for evaluating the independent prognostic value of PPAR signature; (c) ROC curve analyses of the clinical characteristics and risk score.

cancer-related pathways including focal adhesion, pathways in cancer, WNT signaling pathway, TGF-β signaling pathway, bladder cancer, and MAPK signaling pathway. Therefore, PPAR signature could serve as a predictor for BLCA prognosis and might play a critical role in BLCA biology.

Numerous evidences have proven the crucial influence of tumor microenvironment upon the progression, prognosis, and therapy in BLCA. The higher infiltration level of CD8+ T cells was positively correlated with better prognosis [27–29]. Increasing evidence suggests that M2 macrophages could accelerate the malignant progression and distant metastasis [30, 31]. Furthermore, M2 macrophages were also correlated with the immunosuppressive microenvironment and unfavorable prognosis [32, 33]. T cells gamma delta, also known as $\gamma\delta$ T cells, were characterized with the antigen specificity and NK-like cytotoxicity. $\gamma\delta$ T cells can recognize and present tumor antigen in a major histocompatibility complex- (MHC-) independent manner, and activated $\gamma\delta$ T cells could enhance the antitumor activity of adaptive immune cells [34, 35]. In addition, $\gamma\delta$ T cells also have been reported to be related to favorable prognosis [36]. Nevertheless, some studies have reported that $\gamma\delta$ T cells facilitated tumor progression by promoting angiogenesis, recruiting inhibitory cells, and enhancing the apoptosis of antitumor immune cells [37–39]. $\gamma\delta$ T cells played an important role in antitumor activity of intravesical bacillus Calmette-Guérin (BCG) against BLCA [40, 41]. $\gamma\delta$ T cells also can heighten the carboplatin-induced cytotoxicity to BLCA [42]. Our results also suggested that PPAR signature displayed the strong correlation with tumor microenvironment as well as immune cell infiltration. Furthermore, the results showed that CD8+ T cell, Tregs, M0 and M2 macrophages, plasma cell, and T cells gamma delta were significantly distinct between high- and low-risk groups. Patients with high PPARscore had more proportions of M0 and M2 macrophages while patients with low PPARscore had more proportions of CD8+ T cell, plasma cell, and T cells gamma delta. In addition, immune checkpoints including PD-L1, HAVCR2, TIGIT, and LAG3 in the high-risk group were also higher than those in the low-risk group, which indicated that patients in the high-risk group might belong to the "hot" tumor that was tended to benefit from immune checkpoint inhibitor therapy [43]. Furthermore, based on the results of the GDSC database, patients in the high-risk group also might benefit from chemotherapy drugs including Bleomycin, Mitomycin C, Gemcitabine, Cyclopamine, Docetaxel, Cisplatin, Paclitaxel, Rapamycin, Parthenolide, Vinblastine, and Doxorubicin.

We found that eleven small molecule drugs, such as vorinostat, cinchonine, helveticoside, lanatoside C, tiapride, idoxuridine, niclosamide, ampicillin, epitiostanol, pyrimethamine, and cephaeline, could improve the therapeutic effect of BLCA patients. Pyrimethamine, an antimalarial drug, has been observed to inhibit the proliferation and induce the apoptosis in various cancers [44–46].

Of course, there were also several disadvantages in our study. On one hand, the prognostic PPAR signature was constructed and validated only by public database and retrospective research and required to be verified through a prospective trial. On the other hand, the molecular mechanisms of PPAR signature in BLCA should be further validated by in vivo or in vitro experiments.

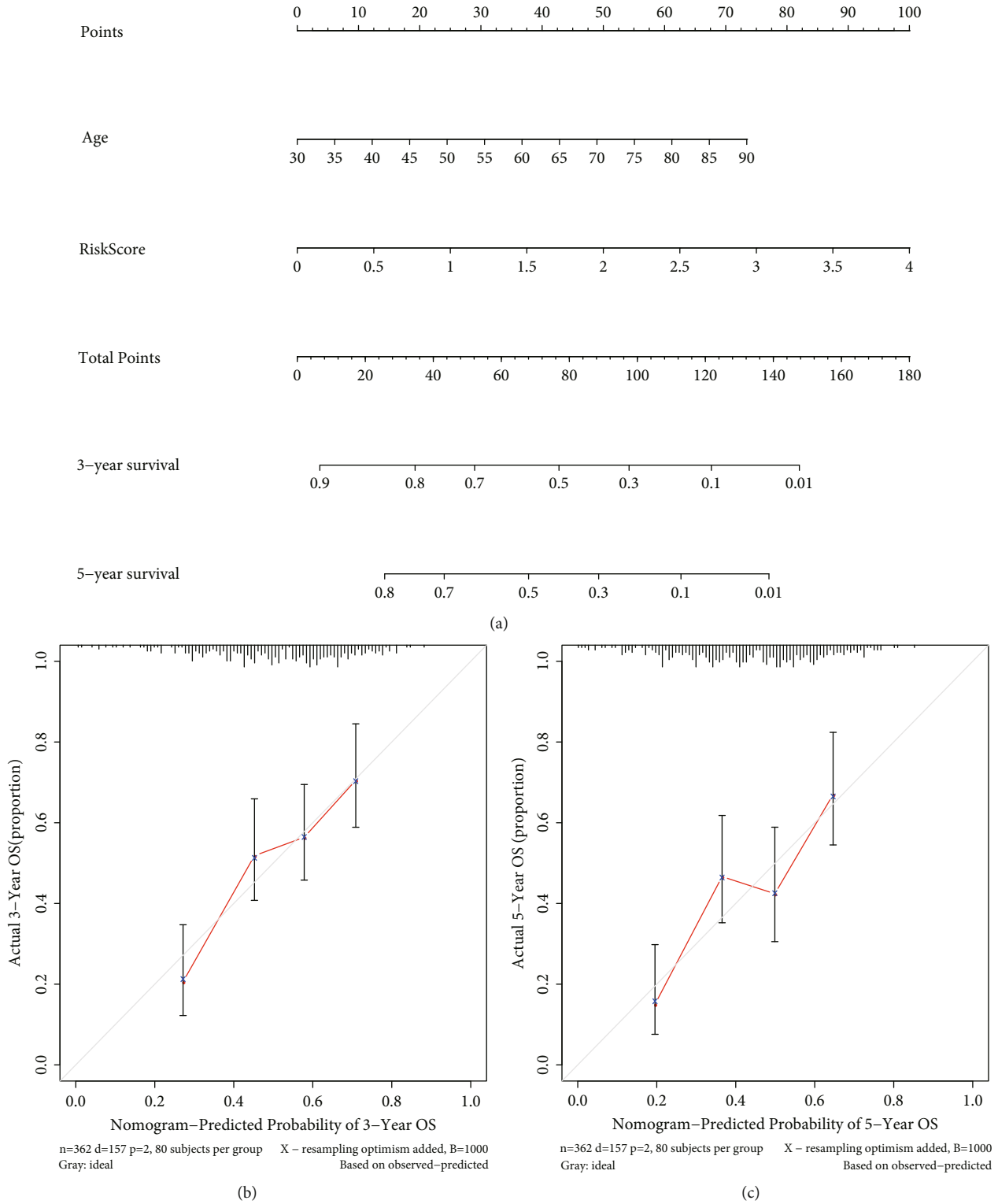

Figure 10: Establishment of the nomogram in the TCGA dataset. (a) Nomogram based on the PPARscore and age; (b) the 3-year calibration plot for the nomogram; (c) the 5-year calibration plot for the nomogram.

5. Conclusion

We comprehensively explored the clinical significance of PPAR-targeted genes and constructed and validated a novel PPAR signature, which showed the excellent performance in predicting prognosis and chemotherapy sensitivity of BLCA patients. Furthermore, we also investigated the correlation between PPAR signature and tumor microenvironment. Finally, several small molecule drugs were identified for the treatments of BLCA patients. All these results uncovered the crucial role of PPAR in BLCA progression and provided novel directions for BLCA therapeutic intervention.

Data Availability

The RNA-sequencing data and clinical characteristic information of patients with BLCA were acquired from the TCGA database (https://gdc-portal.nci.nih.gov/). In addition, validation datasets (GSE13507 and GSE32894) were originated from the GEO database (https://www.ncbi.nlm.nih.gov/geo/). PPAR-targeted genes were obtained from the PPARgene database (http://www.ppargene.org/).

Conflicts of Interest

There is no competing interest.

Authors' Contributions

KZ, LX, and WD designed the research study. LX and WD took responsibility for statistical analyses. KZ wrote the manuscript. WG and BF evaluated and revised the manuscript. All authors read and approved the final manuscript. Ke Zhu and Wen Deng contributed equally to this work.

Acknowledgments

This work was supported by the National Natural Science Foundation of China (No: 81960512).

Supplementary Materials

Supplementary 1. Supplementary Figure 1: functional enrichment analyses of differentially expressed PPAR-targeted genes (DEPPARGs). (A) GO analysis; (B) KEGG pathway analysis. GO: Gene Ontology; KEGG: Kyoto Encyclopedia of Genes and Genomes.

Supplementary 2. Supplementary Figure 2: PCA and *t*-SNE analyses of BLCA patients between the high- and low-risk groups. (A) PCA analysis in the TCGA dataset; (B) *t*-SNE analysis in the TCGA dataset; (C) PCA analysis in the GSE13507 dataset; (D) *t*-SNE analysis in the GSE13507 dataset; (E) PCA analysis in the GSE32894 dataset; (F) *t*-SNE analysis in the GSE32894 dataset. PCA: principal component analysis; *t*-SNE: *t*-distributed stochastic neighbor embedding.

Supplementary 3. Supplementary Figure 3: the potential pathways by gene set enrichment analysis (GSEA) between the high- and low-risk groups.

Supplementary 4. Supplementary Figure 4: the correlation between the risk score and immune cell infiltration, including M0 macrophage, M2 macrophage, CD8+ T cells, Tregs, gamma delta T cells, and plasma cells.

Supplementary 5. Supplementary Figure 5: the expression of key immune checkpoint genes between high- and low-risk groups.

Supplementary 6. Supplementary Figure 6: Kaplan-Meier curve analyses showed the overall survival stratified by age, gender, TNM stage, grade, N stage, and T stage between the high-risk and low-risk groups.

References

[1] H. Sung, J. Ferlay, R. L. Siegel et al., "Global cancer statistics 2020: GLOBOCAN estimates of incidence and mortality worldwide for 36 cancers in 185 countries," *CA: A Cancer Journal for Clinicians*, vol. 71, no. 3, pp. 209–249, 2021.

[2] A. M. Kamat, N. M. Hahn, J. A. Efstathiou et al., "Bladder cancer," *The Lancet.*, vol. 388, no. 10061, pp. 2796–2810, 2016.

[3] J. Youssef and M. Badr, "Peroxisome proliferator-activated receptors and cancer: challenges and opportunities," *British Journal of Pharmacology*, vol. 164, no. 1, pp. 68–82, 2011.

[4] R. Huang, J. Zhang, M. Li et al., "The role of peroxisome proliferator-activated receptors (PPARs) in pan-cancer," *PPAR Research*, vol. 2020, 6527519 pages, 2020.

[5] S. Kersten, B. Desvergne, and W. Wahli, "Roles of PPARs in health and disease," *Nature*, vol. 405, no. 6785, pp. 421–424, 2000.

[6] Y. Xu, X. Li, Y. Han et al., "A new prognostic risk model based on PPAR pathway-related genes in kidney renal clear cell carcinoma," *PPAR Research*, vol. 2020, 6937413 pages, 2020.

[7] D. Bishop-Bailey, "PPARs and angiogenesis," *Biochemical Society Transactions*, vol. 39, no. 6, pp. 1601–1605, 2011.

[8] H. S. Cheng, Y. S. Yip, E. K. Y. Lim, W. Wahli, and N. S. Tan, "PPARs and tumor microenvironment: the emerging roles of the metabolic master regulators in tumor stromal–epithelial crosstalk and carcinogenesis," *Cancers (Basel).*, vol. 13, no. 9, p. 2153, 2021.

[9] J. H. Chung, A. Y. Seo, S. W. Chung et al., "Molecular mechanism of PPAR in the regulation of age-related inflammation," *Ageing Research Reviews*, vol. 7, no. 2, pp. 126–136, 2008.

[10] J. M. Peters, Y. M. Shah, and F. J. Gonzalez, "The role of peroxisome proliferator-activated receptors in carcinogenesis and chemoprevention," *Nature Reviews. Cancer*, vol. 12, no. 3, pp. 181–195, 2012.

[11] I. Takada and M. Makishima, "Peroxisome proliferator-activated receptor agonists and antagonists: a patent review (2014-present)," *Expert Opinion on Therapeutic Patents*, vol. 30, no. 1, pp. 1–13, 2020.

[12] L. Fang, M. Zhang, Y. Li, Y. Liu, Q. Cui, and N. Wang, "PPARgene: a database of experimentally verified and computationally predicted PPAR target genes," *PPAR Research*, vol. 2016, 6042166 pages, 2016.

[13] V. Vantaku, J. Dong, C. R. Ambati et al., "Multi-omics integration analysis robustly predicts high-grade patient survival and identifies CPT1B effect on fatty acid metabolism in bladder cancer," *Clinical Cancer Research*, vol. 25, no. 12, pp. 3689–3701, 2019.

[14] L. Kasikova, M. Hensler, I. Truxova et al., "Calreticulin exposure correlates with robust adaptive antitumor immunity and favorable prognosis in ovarian carcinoma patients," *Journal for Immunotherapy of Cancer*, vol. 7, no. 1, p. 312, 2019.

[15] J. Fucikova, E. Becht, K. Iribarren et al., "Calreticulin expression in human non–small cell lung cancers correlates with increased accumulation of antitumor immune cells and favorable prognosis," *Cancer Research*, vol. 76, no. 7, pp. 1746–1756, 2016.

[16] G. Stoll, K. Iribarren, J. Michels et al., "Calreticulin expression: interaction with the immune infiltrate and impact on survival in patients with ovarian and non-small cell lung cancer," *Oncoimmunology.*, vol. 5, no. 7, article e1177692, 2016.

[17] R.-Q. Peng, Y.-B. Chen, Y. Ding et al., "Expression of calreticulin is associated with infiltration of T-cells in stage IIIB colon cancer," *World Journal of Gastroenterology*, vol. 16, no. 19, pp. 2428–2434, 2010.

[18] L. Liu, J. Hu, Y. Wang et al., "Establishment of a novel risk score model by comprehensively analyzing the immunogen database of bladder cancer to indicate clinical significance and predict prognosis," *Aging (Albany NY)*, vol. 12, no. 12, pp. 11967–11989, 2020.

[19] M. P. Chao, S. Jaiswal, R. Weissman-Tsukamoto et al., "Calreticulin is the dominant pro-phagocytic signal on multiple human cancers and is counterbalanced by CD47," *Science Translational Medicine*, vol. 2, no. 63, p. 63ra94, 2010.

[20] J. Liu, H. Ma, L. Meng et al., "Construction and external validation of a ferroptosis-related gene signature of predictive value for the overall survival in bladder cancer," *Frontiers in Molecular Biosciences*, vol. 8, article 675651, 2021.

[21] Y. Jiang, C. Mao, R. Yang et al., "EGLN1/c-Myc induced lymphoid-specific helicase inhibits ferroptosis through lipid metabolic gene expression changes," *Theranostics.*, vol. 7, no. 13, pp. 3293–3305, 2017.

[22] B. Chen, J. Wang, D. Dai et al., "AHNAK suppresses tumour proliferation and invasion by targeting multiple pathways in triple-negative breast cancer," *Journal of Experimental & Clinical Cancer Research*, vol. 36, no. 1, p. 65, 2017.

[23] E. Shen, X. Wang, X. Liu et al., "MicroRNA-93-5p promotes epithelial-mesenchymal transition in gastric cancer by repressing tumor suppressor AHNAK expression," *Cancer Cell International*, vol. 20, no. 1, p. 76, 2020.

[24] J. Shankar, A. Messenberg, J. Chan, T. M. Underhill, L. J. Foster, and I. R. Nabi, "Pseudopodial actin dynamics control epithelial-mesenchymal transition in metastatic cancer cells," *Cancer Research*, vol. 70, no. 9, pp. 3780–3790, 2010.

[25] W.-C. Cho, J.-E. Jang, K.-H. Kim, B.-C. Yoo, and J.-L. Ku, "SORBS1 serves a metastatic role via suppression of AHNAK in colorectal cancer cell lines," *International Journal of Oncology*, vol. 56, no. 5, pp. 1140–1151, 2020.

[26] X. Xiang, S. Langlois, M.-E. St-Pierre et al., "Identification of pannexin 1-regulated genes, interactome, and pathways in rhabdomyosarcoma and its tumor inhibitory interaction with AHNAK," *Oncogene*, vol. 40, no. 10, pp. 1868–1883, 2021.

[27] P. Sharma, Y. Shen, S. Wen et al., "CD8 tumor-infiltrating lymphocytes are predictive of survival in muscle-invasive urothelial carcinoma," *Proceedings of the National Academy of Sciences of the United States of America*, vol. 104, no. 10, pp. 3967–3972, 2007.

[28] A. M. van der Leun, D. S. Thommen, and T. N. Schumacher, "$CD8^+$ T cell states in human cancer: insights from single-cell analysis," *Nature Reviews. Cancer*, vol. 20, no. 4, pp. 218–232, 2020.

[29] S. van Wilpe, E. C. F. Gerretsen, A. G. van der Heijden, I. J. M. de Vries, W. R. Gerritsen, and N. Mehra, "Prognostic and predictive value of tumor-infiltrating immune cells in urothelial cancer of the bladder," *Cancers (Basel).*, vol. 12, no. 9, p. 2692, 2020.

[30] M. B. Maniecki, A. Etzerodt, B. P. Ulhøi et al., "Tumor-promoting macrophages induce the expression of the macrophage-specific receptor CD163 in malignant cells," *International Journal of Cancer*, vol. 131, no. 10, pp. 2320–2331, 2012.

[31] H. Wu, X. Zhang, D. Han, J. Cao, and J. Tian, "Tumour-associated macrophages mediate the invasion and metastasis of bladder cancer cells through CXCL8," *Peer J.*, vol. 8, p. e8721, 2020.

[32] Z.-F. Wen, H. Liu, R. Gao et al., "Tumor cell-released autophagosomes (TRAPs) promote immunosuppression through induction of M2-like macrophages with increased expression of PD-L1," *Journal for Immunotherapy of Cancer*, vol. 6, no. 1, p. 151, 2018.

[33] Y. Qi, Y. Chang, Z. Wang et al., "Tumor-associated macrophages expressing galectin-9 identify immunoevasive subtype muscle-invasive bladder cancer with poor prognosis but favorable adjuvant chemotherapeutic response," *Cancer Immunology, Immunotherapy*, vol. 68, no. 12, pp. 2067–2080, 2019.

[34] C. R. Willcox, F. Mohammed, and B. E. Willcox, "The distinct MHC-unrestricted immunobiology of innate-like and adaptive-like human $\gamma\delta$ T cell subsets—nature's CAR-T cells," *Immunological Reviews*, vol. 298, no. 1, pp. 25–46, 2020.

[35] Y. Li, G. Li, J. Zhang, X. Wu, and X. Chen, "The dual roles of human $\gamma\delta$ T cells: anti-tumor or tumor-promoting," *Frontiers in Immunology*, vol. 11, article 619954, 2021.

[36] A. J. Gentles, A. M. Newman, C. L. Liu et al., "The prognostic landscape of genes and infiltrating immune cells across human cancers," *Nature Medicine*, vol. 21, no. 8, pp. 938–945, 2015.

[37] J. H. Park and H. K. Lee, "Function of $\gamma\delta$ T cells in tumor immunology and their application to cancer therapy," *Experimental & Molecular Medicine*, vol. 53, no. 3, pp. 318–327, 2021.

[38] J. Yan and J. Huang, "Innate $\gamma\delta$T17 cells convert cancer-elicited inflammation into immunosuppression through myeloid-derived suppressor cells," *Oncoimmunology.*, vol. 3, no. 8, article e953423, 2014.

[39] D. Daley, C. Zambirinis, L. Seifert et al., "$\gamma\delta$ T cells support pancreatic oncogenesis by restraining $\alpha\beta$ T cell activation," *Cell*, vol. 166, no. 6, pp. 1485–1499.e15, 2016.

[40] N. Ji, N. Mukherjee, E. E. Morales et al., "Percutaneous BCG enhances innate effector antitumor cytotoxicity during treatment of bladder cancer: a translational clinical trial," *Oncoimmunology.*, vol. 8, no. 8, p. 1614857, 2019.

[41] N. Ji, N. Mukherjee, R. M. Reyes et al., "Rapamycin enhances BCG-specific $\gamma\delta$ T cells during intravesical BCG therapy for non-muscle invasive bladder cancer: a randomized, double-blind study," *Journal for Immunotherapy of Cancer*, vol. 9, no. 3, article e001941, 2021.

[42] Y. PAN, Y. H. CHIU, S. C. CHIU et al., "Gamma/delta T-cells enhance carboplatin-induced cytotoxicity towards advanced

bladder cancer cells," *Anticancer Research*, vol. 40, no. 9, pp. 5221–5227, 2020.

[43] Y. Zhang and L. Chen, "Classification of advanced human cancers based on tumor immunity in the microenvironment (TIME) for cancer immunotherapy," *JAMA Oncology*, vol. 2, no. 11, pp. 1403-1404, 2016.

[44] M. Lapidot, A. E. Case, D. Larios et al., "Inhibitors of the transcription factor STAT3 decrease growth and induce immune response genes in models of malignant pleural mesothelioma (MPM)," *Cancers (Basel).*, vol. 13, no. 1, p. 7, 2021.

[45] X. Zhou, J. Zhang, X. Hu et al., "Pyrimethamine elicits antitumor effects on prostate cancer by inhibiting the p38-NF-κB pathway," *Frontiers in Pharmacology*, vol. 11, p. 758, 2020.

[46] M.-X. Lin, S.-H. Lin, C.-C. Lin, C.-C. Yang, and S.-Y. Yuan, "In vitro and in vivo antitumor effects of pyrimethamine on non-small cell lung cancers," *Anticancer Research*, vol. 38, no. 6, pp. 3435–3445, 2018.